Contract No:

This document was prepared in conjunction with work accomplished under Contract No. DE-AC09-08SR22470 with the U.S. Department of Energy (DOE) Office of Environmental Management (EM).

Disclaimer:

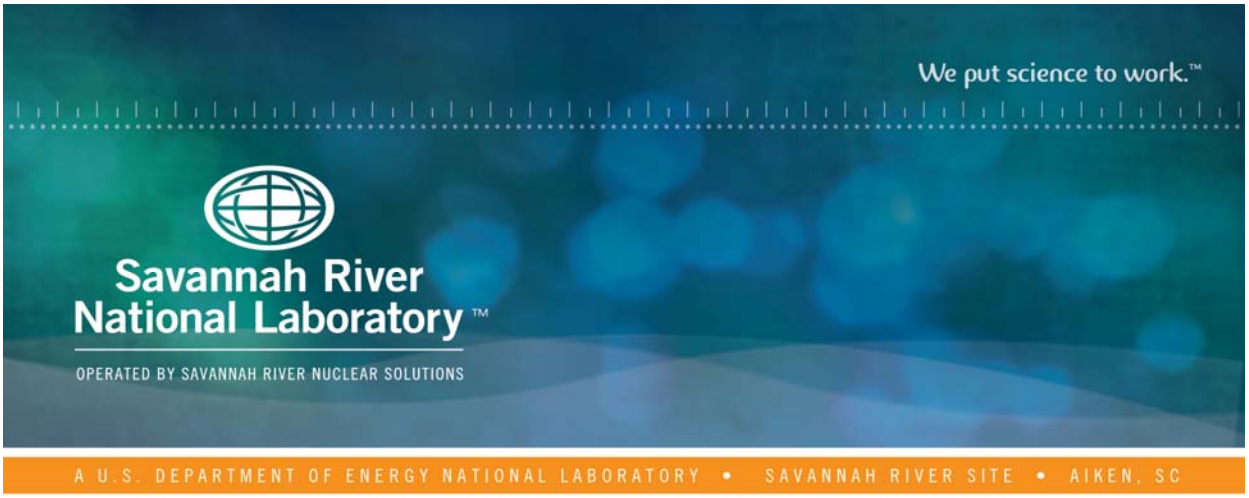

Retained Hydrogen Literature Study for DWPF

M. R. Poirier

E. K. Hansen

September 2019

SRNL-STI-2019-00394, Revision 0

DISCLAIMER

Printed in the United States of America

Prepared for
U.S. Department of Energy

SRNL-STI-2019-00394
Revision 0

Keywords: *Hydrogen, Mixing, DWPF*

Retention: *Permanent*

Retained Hydrogen Literature Study for DWPF

M. R. Poirier
E. K. Hansen

September, 2019

Prepared for the U.S. Department of Energy under contract number DE-AC09-08SR22470.

Savannah River National Laboratory™
OPERATED BY SAVANNAH RIVER NUCLEAR SOLUTIONS

REVIEWS AND APPROVALS

AUTHORS:

M. R. Poirier, Advanced Characterization and Processing Date

E. K. Hansen, Waste Form Processing Technologies Date

TECHNICAL REVIEW:

M. E. Stone, Waste Form Processing Technologies, Reviewed per E7 2.60 Date

M. R. Duignan, Advanced Characterization and Processing, Reviewed per E7, 2.60 Date

APPROVAL:

F. M. Pennebaker, SRNL Customer Program Manager for SRR Support Chemical Processing Technologies Date

S. D. Fink, Director, Chemical Processing Technologies Date

E. J. Freed, Manager, DWPF/Saltstone/Facility Engineering Date

EXECUTIVE SUMMARY

During Defense Waste Processing Facility (DWPF) operation in the Slurry Receipt and Adjustment Tank (SRAT) and the Slurry Mix Evaporator (SME), hydrogen is primarily produced by radiolysis and catalytic generation. The hydrogen is released from the sludge by agitation and removed from the vapor space by purging with air. Upon loss of agitation, the hydrogen begins accumulating in the sludge, and releases rapidly upon the resumption of agitation. If enough hydrogen accumulated in the sludge, and released rapidly upon the start of agitation, the hydrogen concentration in the vapor space could exceed the lower flammability limit (4 vol %).

Savannah River Remediation (SRR) currently manages the risk for retained hydrogen in the DWPF vessels by implementing a Retained Hydrogen Program. The program primarily relies on the timely operation of vessel agitators to ensure that the retained hydrogen eruptions that could lead to flammable vapor spaces do not occur. The current program relies on conservative assumptions concerning gas release and retention (e.g., instantaneous release, conservative hydrogen bubble fraction, no release during quiescent periods) to develop allowable vessel quiescent times (Q-times). SRR would like to relax the conservative assumptions to the Retained Hydrogen Program and allow the Retained Hydrogen Program to extend past Sludge Batch 9. Relaxing the assumptions could potentially allow longer Q-times during agitator stoppages.

SRR requested Savannah River National Laboratory (SRNL) personnel to perform a literature study to extract industry data pertaining to retained hydrogen and apply it to the DWPF process. The authors conducted a review of the technical literature, including work from the Savannah River Site (SRS), SRNL, the Hanford site, Pacific Northwest National Laboratory (PNNL), and the Sellafield site to identify literature describing the retention and release of gases with non-Newtonian slurries. The study was undertaken with the knowledge that SRS wastes are unique which makes using non-SRS data challenging. The literature search focused on the following topics:

- Mixing or blend time in Newtonian and non-Newtonian fluids
- Quiescent release of gas from an unagitated non-Newtonian fluid
- Release of gas from an agitated non-Newtonian fluid
- Changes in fluid rheology as a function of settling time

The review of the technical literature describing the blending of Newtonian fluids and non-Newtonian fluids shows the mixing/blending to be a very fast process. In most instances the mixing time was less than 2 minutes. Investigating the mixing time in the SRAT and SME is unlikely to provide the data needed to relax the assumptions on instantaneous release of hydrogen upon the start of agitation, and the focus of the investigation is on hydrogen release rather than mixing time. Therefore, no further investigation of mixing/blending time is recommended.

The literature on gas release from non-Newtonian fluids under quiescent conditions suggests a critical yield stress exists above which gas bubbles will not be released and below which gas bubbles will be released. The search also identified work in which hydrogen retention was a function of depth, but the work did not discuss the mechanism for the effect. Several investigators observed quiescent releases of gas bubbles. Included in the work observing quiescent release of hydrogen gas is data from the DWPF, SRNL data from DWPF sludge batch qualification, and the SRS Tank Farm. In assessing the quiescent release of gas from DWPF slurries, the slurry property of importance is the shear strength.

SRNL sludge batch qualification testing showed retained hydrogen was released over several minutes rather than instantaneously upon startup of agitation. Tank Farm data measuring the release of hydrogen during mixing with slurry pumps showed the hydrogen release to occur over several hours rather than instantaneously. Because of differences in agitation intensity, agitation method, vessel volume, headspace

volume, purge rate, and power input, this data cannot be directly applied to the DWPF, but it is important to note that hydrogen is released over a finite time, rather than instantaneously.

Previous work by SRNL and PNNL has measured the rheology of Hanford sludge, and shown the rheology (i.e., yield stress or shear strength) to increase as the sludge is allowed to settle. Changes in sludge rheology need to be considered when assessing changes to the DWPF retained hydrogen program.

A comparison of buoyancy and inertial forces under SRAT operating conditions (1 – 10 Pa yield stress, 1.38 g/mL density, 65 or 130 rpm, 9,000 gallons of feed) on the bubbles (approximated as 300 micron diameter) found the inertial forces to be more than 350,000 times larger than the buoyancy forces. With this ratio of forces, the gas bubbles generated will follow the fluid motion in the SRAT, and only release when they reach the slurry-vapor interface.

An informal Lattice Boltzmann Computation Fluid Dynamics calculation was performed on a SRAT type vessel. The liquid was assumed to have a density of 1 g/mL and a viscosity of 20 cP. In the simulation, approximately 50% of the bubbles were released to the vapor space over ~80 seconds. The simulation showed the bubbles to follow the liquid flow, and only release when they reached the liquid surface.

The authors recommend the following work be performed to assess the conservatism in the retained hydrogen program.

- Measuring quiescent hydrogen release from actual SRS waste.
- Measuring agitated hydrogen release from actual SRS waste.
- Modeling gas bubble release from SRS waste using Lattice-Boltzmann CFD software.
- Analyzing DWPF process data to better understand release rates at the DWPF.
- Conducting gas release tests with simulant to assist in the design of actual waste tests and the validation of the Lattice-Boltzmann CFD model.
- Performing rheology measurements to understand the impact of settling time on slurry rheology.
- Testing performed should include feeds representative of the DWPF contents with the glycolic acid flowsheet.

TABLE OF CONTENTS

LIST OF TABLES

LIST OF FIGURES

LIST OF ABBREVIATIONS

ARP	Actinide Removal Process
Bn	Bingham number
C	Concentration
C_0	Initial concentration
CFD	Computational Fluid Dynamics
CPC	Chemical Processing Cell
D	Impeller Diameter
d	Bubble diameter
D_{32}	Sauter mean diameter of gas bubble
Di	Inner diameter of annulus
D_o	Outer diameter of annulus
D_j	Jet discharge nozzle diameter
DOE	Department of Energy
dp	Bubble diameter
DWPF	Defense Waste Processing Facility
g	Gravitational acceleration
GC	Gas Chromatograph
H	Height
HGR	Hydrogen Generation Rate
HLW	High-Level Waste
K	Herschel-Bulkley consistency
LFL	Lower Flammability Limit
MCU	Modular Caustic Side Solvent Extraction Unit
MST	Monosodium titanate
N	Impeller Speed
N	Power index
Np	Power Number
N_Q	Flow Number
PNNL	Pacific Northwest National Laboratory
P/V	Power per Unit Volume
Q	Quiescent Release rate
Q	Gas purge rate
R	Pump cleaning radius
Re	Reynolds number

R_B	Bubble radius
SCCM	Standard cubic centimeters per minute
SCFM	Standard Cubic Feet per Minute
SME	Slurry Mix Evaporator
SRAT	Sludge Receipt and Adjustment Tank
SRNL	Savannah River National Laboratory
SRS	Savannah River Site
SRR	Savannah River Remediation
T	Tank Diameter
t	Time
TAR	Technical Assistance Request
V	Vessel Volume
V	Head space volume
V_B	Bubble volume
V_j	Jet nozzle velocity
Y	Yield parameter
v	Bubble rise velocity
V_{rise}	Bubble rise velocity
ρ	Density
$\Delta\rho$	Density difference
Θ	Mixing/Blending Time
τ_B	Bingham shear stress
τ_{BP}	Bingham plastic yield stress
τ_{HB}	Herschel Bulkley yield stress
τ_{max}	Maximum yield stress
τ_y	Yield stress
η_{BP}	Plastic viscosity
γ	Shear rate
σ	Surface tension
ν	Kinematic viscosity
μ	Viscosity
ε_H	Gas hold up fraction

1.0 Introduction

1.1 Background

Vitrification of High Level Waste (HLW) at the Savannah River Site (SRS) Defense Waste Processing Facility (DWPF) requires pretreatment of the sludge in the Chemical Processing Cell (CPC), which consists of the Sludge Receipt and Adjustment Tank (SRAT) and the Slurry Mix Evaporator (SME).

The SRAT receives washed sludge slurry from the SRS Tank Farm, concentrated sludge and monosodium titanate (MST) slurry from the Actinide Removal Process (ARP), and strip effluent from the Modular Caustic Side Solvent Extraction Unit (MCU).[a] The washed sludge contains 13 – 19 wt % total solids with a yield stress of 1.5 – 5 Pa and a consistency of 5 – 12 cP.[1] The concentrated sludge/MST slurry insoluble solids content is variable and can contain up to 10 wt % insoluble solids with varying yield stress. The strip effluent contains no solid particles and has no yield stress. These streams are mixed in variable ratios in the SRAT to produce a slurry with yield stress of 1.5 – 5 Pa and consistency of 5 – 12 cP. The SRAT contents are heated to 93˚C and 50 wt % nitric acid and 90 wt % formic acid are added to the vessel. The formic acid/nitric acid acidifies the sludge to reduce its yield stress, reduces the valence of manganese to reduce foaming, reacts with the mercury to form elemental mercury which is steam stripped from the SRAT, destroys nitrite and carbonate, and adjusts the formate-nitrate balance to produce a melter feed that meets the Reduction/Oxidization potential for melter feed. After concentration by evaporation, the SRAT contents are boiled under reflux to steam-strip mercury to below 0.45 wt % (solids basis). Strip effluent additions occur at boiling during mercury stripping and replaces some period of reflux boiling.

The SME receives adjusted slurry from the SRAT. Frit is added to the SME contents. Other chemicals may be added to ensure proper processing of the sludge and melter. The SME is nominally designed to process contents having a yield stress of 2.5 – 15 Pa, and a consistency of 10 – 40 cP.[1] Nitric acid or formic acid may be added to the SME to adjust the slurry redox or rheology. The SME evaporates the frit-sludge-sludge/MST slurry to produce a melter feed containing approximately 40 - 45 wt % insoluble solids.

Hydrogen is produced by the catalytic decomposition of formic acid and the radiolytic decomposition of water in the SRAT and SME. To maintain the headspace in the SRAT and SME below the flammability limit, the headspace is purged with air. The DWPF will be implementing a glycolic acid flowsheet, which will reduce the catalytic hydrogen generation rate, but the principles and concerns with hydrogen retention and release will still apply.

Due to the non-Newtonian rheology of the slurries, the loss of agitation during a process failure or system outage would allow some fraction of the generated hydrogen to be retained until agitation is resumed. If enough hydrogen has been retained by the sludge during loss of agitation, it could release rapidly upon the restart of agitation and create a flammable mixture in the vapor space.

The DWPF SRAT and SME are cylindrical vessels that are 12 ft diameter and 13 feet tall, with a volume of 11,000 gallons. The maximum working volume of sludge is 9,000 gallons with a minimum vapor space of 2,000 gallons. The vessels contain a cooling coil assembly that is composed of three sets of coils. The coils surround the agitator and the assemblies have diameters of 46.5, 52.5, and 58.5 inches. The coils are constructed of 2 inch schedule 40 pipe. The cooling coil assembly forms a draft tube which is ~45 inches inner diameter and ~60 inches outer diameter. Most of the fluid motion through the coil assembly will be downward, but some of it may pass through the coil assembly. The vessels are mixed with two impellers, a 3 ft diameter 4 bladed radial flow impeller near the bottom of the cooling coil assembly, and a 3 ft diameter

[a] Following startup of the Salt Waste Processing Facility (SWPF), the DWPF will received concentrated sludge and MST slurry and strip effluent from the SWPF.

3 bladed axial flow impeller near the top of the cooling coil assembly.[1] The power numbers (N_p) for these impellers are 4 and 0.7 respectively and are for fully baffled and turbulent conditions around the impeller.[2] The impeller speed is either 65 rpm or 130 rpm. Assuming a fluid density of 1.38 g/mL, and an impeller speed of 130 rpm, the power per unit volume for 9,000 gallons of feed is calculated with equation [1],

$$\frac{P}{V} = \frac{N_p\,\rho\,N^3D^5}{V} = \frac{(4+0.7)\left(1.38\ g/cm^3\right)\left(\frac{130}{60}sec^{-1}\right)^3(91.44\ cm)^5}{9{,}000\ gallons\left(\frac{3785\ cm^3}{gallon}\right)} = 12{,}400\,\frac{g}{cm{\cdot}sec^3} \qquad [1]$$

where ρ is the fluid density, N is the impeller rotation rate, D is the impeller diameter, and V is the fluid volume. The fluid density will vary during the SRAT cycle. The value of 1.38 g/mL was selected to give the largest power per unit volume. Changing the density of the fluid will change the result of the calculation, but it will not change the overall conclusions of the report. For a fluid viscosity of 10 cp, the Reynolds number ($Re = \rho\,N\,D^2/\mu$) is 250,000 at an impeller speed of 130 rpm, and 125,000 at an impeller speed of 65 rpm; both of these conditions are turbulent. Because the fluid density and rheology change during the process, the yield stress, Reynolds number, and power per unit volume will change throughout the process.

Savannah River Remediation (SRR) currently manages the risk for retained hydrogen in the Defense Waste Processing Facility (DWPF) vessels by implementing a Retained Hydrogen Program. The program primarily relies on the timely operation of vessel agitators to ensure that the retained hydrogen eruptions that could lead to flammable vapor spaces do not occur. The current program relies on Sludge Batch 8 Gas Chromatograph data and on conservative assumptions concerning gas release and retention (e.g., instantaneous release, conservative hydrogen bubble fraction, no release during quiescent periods) to develop allowable vessel quiescent times (Q-times).[3] SRR would like to establish more realistic inputs to the Retained Hydrogen Program, and allow the Retained Hydrogen Program to extend past Sludge Batch 9.[4] These more realistic inputs could potentially allow longer Q-times during agitator stoppages.

1.2 Rheological Measurements and Models

Hydrogen gas retention and release is a function of the slurry rheology. The relationship is discussed later in the document. In the DOE complex, the rheology properties of sludge have been measured using either a flow curve or vane method to determine the yield stress of the sludge. The conditions and application of the data from these measurements can be quite different. The flow curve measures the shear stress (or viscosity) as a function of shear rate (typically ranging over a couple of decades) in a rotational rheometer, typically utilizing concentric geometry given the conditions of the sludge. In this case, the fluid is typically loaded into a cup after it has been sufficiently mixed to remove most of the thixotropic characteristics and the flow curve immediately measured. At times, the slurry is kept in the concentric geometry and multiple flow curve measurement are made, to again, remove the thixotropic properties. Hence, a flow curve is that of a moving fluid with much of its thixotropic properties removed and is shear thinning (e.g., as the shear stress goes up, the apparent viscosity goes down). Given the slurries are non-Newtonian with a yield stress, the flow curves at SRS are fit with a Bingham Plastic rheological model (equation [2]) and at other sites, also fitted to the Herchel Bulkley rheological model (equation [3]). The difference between these two models is how the models are fit to the flow curve. Typically for a Bingham Plastic fluid, the linear region of the flow curve, at the higher shear rates, is fit. For the Herchel Bulkley fluid, the complete flow curve is fit. The results from such analysis can be observed in Figure 1 for an Oak Ridge sludge that was analyzed by SRNL at two different undissolved solids concentrations.[5] As the solids concentrations increases, the difference between the two yield stress increases and such is typical. From a mixing or transport calculation, using the Bingham Plastic model is conservative for design. The results from the maximum undissolved solids concentration are compared to the vane measurement in section 3.4

$$\tau_B = \tau_{BP} + \eta_{BP}\dot{\gamma} \quad [2]$$

where: τ_{BP} = Bingham Plastic yield stress (Pa)
η_{BP} = Plastic Viscosity (Pa-s)
$\dot{\gamma}$ = Shear rate (sec^{-1})

$$\tau_H = \tau_{HB} + K\dot{\gamma}^n \quad [3]$$

where: τ_{HB}= Herchel Bulkley yield stress (Pa)
K = consistency (Pa-s^n)
n = power index (unitless)

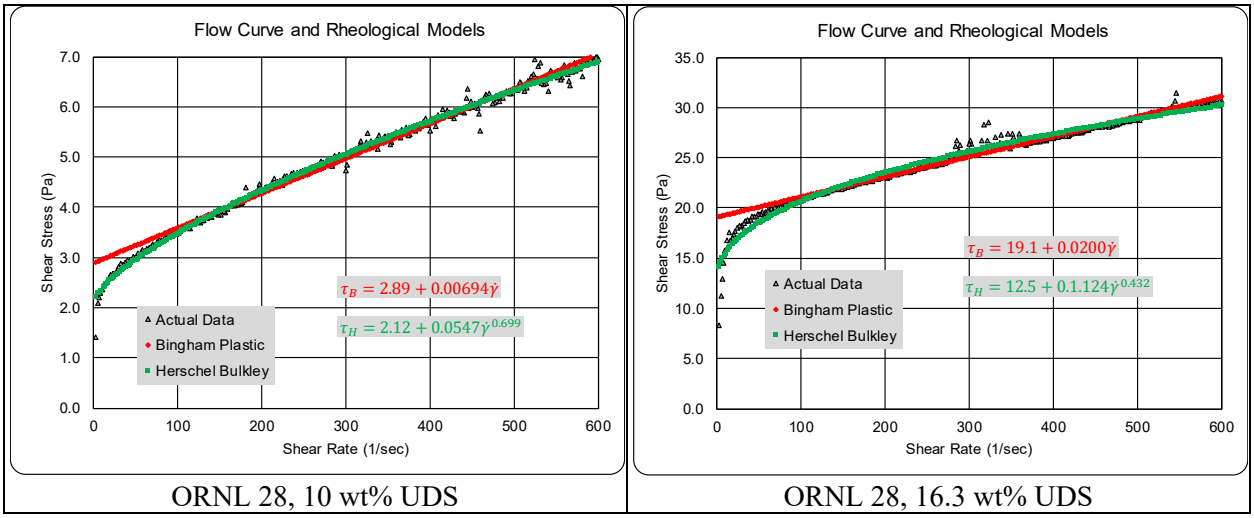

ORNL 28, 10 wt% UDS | ORNL 28, 16.3 wt% UDS

Figure 1. Flow Curve Analysis of ORNL 28 Sample by SRNL

The vane measurements are typically performed when a slurry is allowed to settle for a specific time undisturbed, at which point a vane is inserted and the measurement obtained. As the vane is slowly rotated through the sample, where stress and time are recorded, there typically is an initial linear region (G, called Hookean elastic modulus, Figure 2) and the point of departure from this linear region is call the static yield stress, which is the transition for fully elastic to viscoelastic behavior. At the maximum yield stress (τ_{max},Figure 2), the fluid starts to transition from a viscoelastic to fully viscous. The maximum yield stress is what is typically reported as the settled solids yield stress (shear strength), given this is much easier to determine from such a curve. In almost all cases where the solids have been allowed to settled for at least 24 hours, the settled solids yield stress is greater than that of the flow curve, as expected (see section 3.4). This parameter is typically used by Hanford to assess the settled solids ability to retain gas, given these are the conditions in which the gas resides. Such measurements have not been performed on SRS sludge or melter feed. If the vane measurement is made immediately from a well-mixed sample, results indicate that the vane yield stress (not really a settled solid shear stress) is slightly less than that of the Bingham Plastic flow curve result of the same fluid.[6] Furthermore, it was shown that the yield stress was independent of slurry height, if the slurry was not allowed to settle, indicating that for a well-mixed slurry, rheology is independent of location in the vessel. However, if the slurry was allowed to settle, a settled solids yield stress gradient was formed, with the smallest yield stress at the top and the largest yield stress at the bottom.

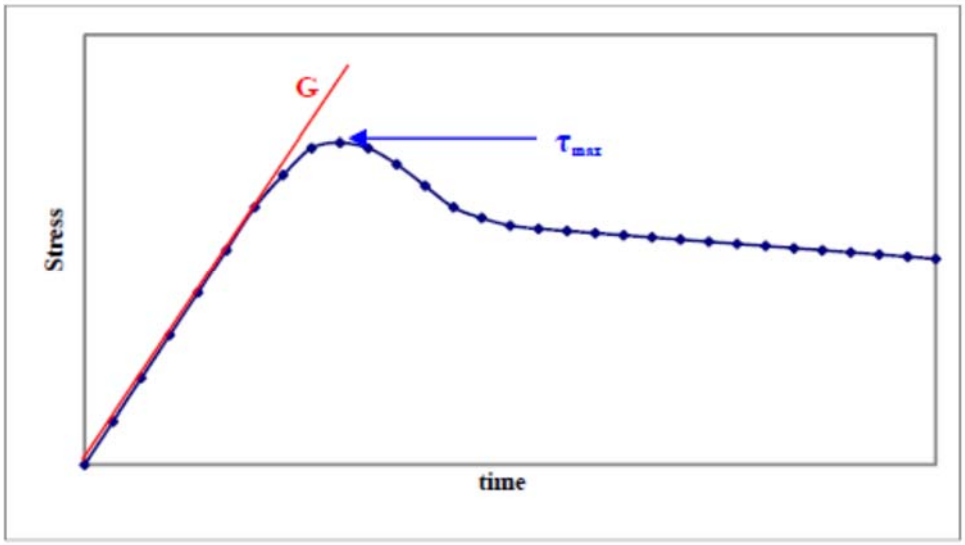

Figure 2. Typical Vane Measurements

SRR requested Savannah River National Laboratory (SRNL) personnel to perform a literature study to extract industry and DOE Complex data pertaining to retained hydrogen and apply it to the DWPF process.[4] The study included published reports from SRS, Hanford, PNNL, Sellafield, and the technical literature, as well as a review of the SRR retained hydrogen program. The survey also looked at other industrial or academic sources of data as well as consulting with acknowledged experts in this arena. This document describes the study, along with recommendations for future testing. Because of the unique nature of the SRS waste (i.e., sludge), the radioactive environment, and the unique mixing environment, finding applicable work in the technical literature is challenging.

2.0 Approach

2.1 Literature Review

The authors conducted a review of the technical literature, including work from SRS, SRNL, the Hanford site, PNNL, and the Sellafield site to identify literature describing the retention and release of gases (including hydrogen) with non-Newtonian slurries. Much of the work performed to investigate gas retention and release for DOE radioactive liquid waste used oxygen rather than hydrogen because of safety concerns, so the investigation looked at the retention and release of other gases as well as hydrogen. The slurries included Bingham plastic fluids, Herschel-Bulkley fluids, and pseudoplastic fluids.

The study was undertaken with the knowledge that SRS wastes are unique which makes using non-SRS data challenging. The literature search focused on the following topics:

- Mixing or blend time[b] in Newtonian and non-Newtonian fluids
- Quiescent release of gas from an unagitated non-Newtonian fluid
- Release of gas from an agitated non-Newtonian fluid
- Changes in fluid rheology due to settling of the slurry

The mixing of Bingham Plastic, Herschel-Bulkley, and pseudoplastic fluids is often described with the cavern model.[7,8,9] The basis of this model is that close to the impeller the shear stresses generated by the

[b] In this document, the term "mixing" refers to the process of combining substances (gas, liquid, or solid) to produce a product with a predetermined degree of homogeneity, and the term "blending" refers to the process of mixing miscible fluids to create a fluid with a predetermined degree of homogeneity. "Blending" is a subset of "mixing".

impeller are greater than the yield stress of the slurry, and the slurry is well mixed. As the distance from the impeller increases, the applied shear stress decreases and if the slurry yield stress is greater than this shear stress, the slurry is stagnant. The model assumes a well-defined boundary between the well-mixed and unmixed regions in the vessel. In practice, a transition region may exist between the two regions. Figure 3 describes the cavern model.

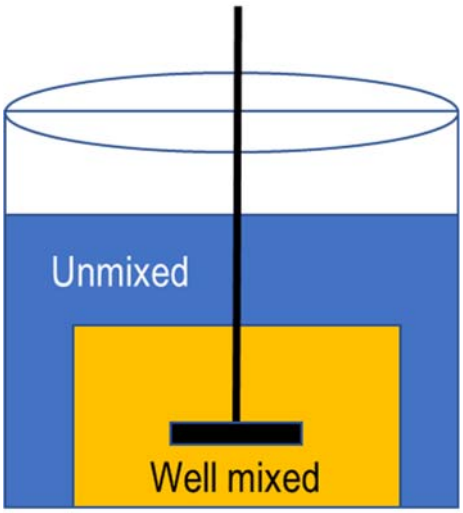

Figure 3. Cavern Model

For the fluid to be well mixed, the mixing cavern should include all the fluid in the vessel. For gas to be more easily released from the vessel, the mixing cavern should extend to the fluid-vapor interface, and to the walls of the vessel. The agitation systems for the SRAT and SME were designed to ensure the well-mixed cavern included the entire working volume of the vessels.

One approach for the literature study was to look at blending of liquids. Blending of liquids, even those with no yield stress and a low viscosity, does not occur instantaneously. The process could take a few seconds, a few minutes, or even hours. If liquid blending does not occur instantaneously, hydrogen release should not occur instantaneously. For a bubble-containing liquid to be well-mixed, the gas bubbles would be distributed throughout the vessel. Under this condition, the bubbles near the surface may be released, but the bubbles in other regions of the vessel would need to be transported to the surface before they could be released. For this reason, the bubble release time would be longer than the liquid blend time. Longer blend times in the SRAT and SME could lead to the relaxation of the assumption that all retained hydrogen is released upon start of agitation. This analysis looked at Newtonian and non-Newtonian fluids.

A second focus of the literature search was to look at published work describing the release of gases from non-Newtonian fluids in a vessel that was not agitated or mixed. The retained hydrogen program assumes that all generated hydrogen is retained while the vessel is quiescent. An objective of this work is to evaluate that assumption. The amount of hydrogen retained in a quiescent vessel is likely a function of the properties of the sludge. This aspect of the literature study looked at previous studies of gas generation and release in quiescent vessels and attempted to ascertain the impact of slurry properties on the amount and rate of gas release.

Another focus was to look at release of gases from non-Newtonian fluids in agitated vessels. While the SRAT and SME are agitated with impellers, this work also looked at vessels that were agitated with pumps, jets, and other devices. The retained hydrogen program assumes that all retained hydrogen is released

instantaneously once agitation starts. In reality, all retained hydrogen should not be released instantaneously. The release could occur in seconds, minutes, or hours. This aspect of the literature study searched for previous work that measured gas release during agitation of non-Newtonian fluids. The goal was to find data or models that would allow calculation of the release rate of hydrogen from the sludge in the DWPF SRAT and SME.

The final area of focus reviewed the influence of settling time on the rheology of slurries. If the agitation stops in the SRAT or SME, the rheology of the slurry in the vessel may change with quiescent time. These changes in rheology with time could change the rate at which the SRAT and SME release hydrogen during quiescent periods, or upon the start of agitation.

2.2 Quality Assurance

The work scope was requested by SRR in a Technical Assistance Request (TAR).[4] The TAR requested a white paper to be written and did not request testing to be performed. The white paper will undergo a technical review and customer review prior to issue.

Requirements for performing reviews of technical reports and the extent of review are established in manual E7 2.60. SRNL documents the extent and type of review using the SRNL Technical Report Design Checklist contained in WSRC-IM-2002-00011, Rev. 2.

3.0 Literature Review

This section will describe some of the key results and observations from the literature search that may provide evidence that the conservative assumption of the gas retention program can be relaxed and allow the Retained Hydrogen Program to extend past Sludge Batch 9 and the Q-times to be increased during agitator stoppages.

3.1 Blending Time

Many of the studies reviewed for this document were conducted at smaller scales than the SRAT and SME. The blending time in the larger vessels could be dramatically different from that observed in smaller vessels and typically the blend time increases with increasing size. In addition, most of the blend tests described started with the vessel at steady state conditions (e.g., agitator providing mixing and flow field fully developed throughout the vessel, considered well-mixed) and added a tracer to measure the blend time. If a tracer is added to a well-mixed vessel, the blend time will be less than if a tracer is added to a vessel prior to the start of mixing. Following an outage, the SRAT and SME will not be agitated, but will start the mixing process from a quiescent state. This difference will lead to a longer mixing time. Finally, many of the tests were conducted under laminar flow conditions (i.e., Re < 5,000 – 10,000), which would have longer blend times.

3.1.1 Newtonian Fluids

Several papers were identified that examined miscible blending in water or low viscosity Newtonian fluids. Derksen computationally investigated blending miscible liquids of different densities starting from a stratified state.[10] The vessel that he modeled contained 4 equally spaced baffles with a width that is 1/10 of the vessel diameter. The contents were mixed with a 45˚ pitch blade turbine with diameter that is 1/3 of the vessel diameter and located above the bottom of the vessel. The two fluids were equal volume in the vessel. The range of Reynolds numbers in the calculations was 3,000 – 12,000, which is much less than the Reynolds number of the SRAT and SME. The work estimated that as little as 30 – 50 impeller revolutions were needed to blend the liquids when the Reynolds number was 6,000, though there were conditions where complete mixing did not occur. At an impeller speed of 65 – 130 rpm, the blend time would be 14 – 46 seconds.

Gogate and Pandit investigated blending of miscible liquids.[11] They conducted their tests in a vessel with a diameter of 31 cm, a liquid height of 60 cm, and four equally spaced baffles. They used disk turbines and pitch blade turbines with diameter of 10 cm and 15 cm. They measured blending by adding sodium chloride solution to water and measuring the change in conductivity. They investigated the impacts of Reynolds number, the volume of tracer solution added, and the density difference between the original solution and the tracer. The measured dimensionless blend time (impeller speed multiplied by the blend time) ranged from 60 – 270.

Kasat and Pandit investigated mixing times in a tank agitated with multiple impellers.[12] Their tank was 30 cm in diameter and 90 cm high. This aspect ratio is much different from the SRAT and SME. The testing used six bladed Rushton turbines and 45˚ pitch blade turbines with an impeller diameter of 10 cm. The impeller speed ranged from 100 – 480 rpm. The tank was filled with water, and a tracer solution of sodium chloride was added. The mixing time was determined by measuring the change in conductivity at select locations in the tank. The Reynolds numbers during testing ranged from 16,000 – 80,000. The measured blend times in the testing were 26 – 107 seconds.

Houcine et al. investigated the effects of tank design and impeller selection on the mixing time in stirred tanks.[13] Their tank was 28.8 cm diameter, the vessel volume was 20 L, the liquid height was 30 – 33.5 cm, the impeller speed was 112 – 716 rpm, and the Reynolds number was 17,200 – 230,000. The tanks had different bottom configurations, and contained four equally spaced baffles with a width of approximately 3 cm. The impellers studied included a Rushton turbine, a 45˚ pitch blade turbine, a MIXEL TT propeller, a MIXEL TTP propeller, and an Ekato INTERMIG propeller. The mixing time was measured by filling the tank with water, adding an electrolyte pulse, and measuring the change in conductivity at three locations in the tank. The measured mixing time was 4 - 18 seconds. The study found that the presence of a draft tube decreased the impeller power consumption but increased the mixing time.

Grenville and Tilton investigated blending of liquids with jets in tanks.[14,15] The tanks ranged in diameter from 0.6 m to 4 m. The blending times ranged from 20 – 5,000 seconds. For the conditions that are most representative of the DWPF SRAT (based on power per unit mass), the blending time was ~ 100 seconds.

The Handbook of Industrial Mixing provides correlations for predicting liquid blend times under turbulent conditions[c] (see equation [4]).[16]

$$\theta_{95} = \frac{5.2T^{1.5}H^{0.5}}{N_p^{1/3}ND^2} \qquad [4]$$

In equation [4], θ_{95} is the 95% blend time, T is the vessel diameter, H is the fluid height, N_p is the impeller power number, N is the impeller rotation rate, and D is the impeller diameter. The correlation is based upon the work of Grenville that conducted testing in tanks of diameter 1 – 6 feet and liquid depth equal to tank diameter, with pitch blade turbines, Rushton turbines, Lightnin A310 hydrofoils, and Chemineer HE3 hydrofoils.[17] With a vessel diameter of 12 ft, a fluid height of 10.5 ft, an impeller power number of 4, an impeller speed of 130 rpm, and an impeller diameter of 3 ft, the calculated blend time is 23 seconds. Since equation [2] is based on testing with tanks smaller than the SRAT and SME, the calculated blend time should be used with caution. However, the likely blend time of these vessels should be on the order of tens of seconds rather than tens of minutes or hours. The blending time calculated with equation [4] matches expectations and DWPF experience.

[c] Reynolds number greater than 5,000 – 10,000

3.1.2 Non-Newtonian Fluids

Ihejirika measured mixing times in yield stress fluids.[18] The mixing time was determined as the time required for the conductivity to be within ± 2% of the final steady state conductivity value after adding the tracer. The vessel used for testing had a diameter of 40 cm, a fluid height of 40 cm, a flat bottom, four baffles with width equal to 10% of tank diameter and equally spaced out, and an impeller diameter of 15.5 cm. The impeller speed was 250 – 700 rpm. The impellers tested were a 45˚ pitch blade turbine, a marine impeller, and a Lightnin A320 hydrofoil. The fluid was an aqueous solution of xanthan gum (0.5, 1.0, and 1.5 wt %). The fluid yield stress was 1.5 – 7.5 Pa when modeled as a Herschel-Bulkley fluid and 5 – 20 Pa when reviewing the flow curve data provided and modeling the fluid as a Bingham plastic. Measured mixing times were 7 – 151 seconds and the condition of mixing was laminar.

Farah Abadi measured mixing times in non-Newtonian fluids.[19] The testing was conducted with solutions of laponite and Carbopol in water in cylindrical glass stirred vessels with diameter of 11.5 cm. The laponite solution is thixotropic. Both fluids were characterized as Herschel-Bulkley fluids having a yield stress of approximately 4 Pa. The testing used pitched blade down pumping, pitched blade up pumping, and Rushton turbine impellers. The impeller diameters were approximately half of the vessel diameter. The liquid height was equal to the vessel diameter. The testing determined the area of the well-mixed cavern as a function of time under laminar and transitional regimes (Re = 7 – 158). The work found the mixing cavern to reach steady state in 10 – 150 seconds. In most of the tests, the cavern region reached 80% of its steady-state value within 20 seconds. These results suggest that if the mixing cavern in the SRAT and SME includes the entire contents of the vessel, the cavern should be large enough to begin releasing hydrogen in a short time. Caution should be used in applying these results to the SRAT and SME given the mixing regimes analyzed are not turbulent, the fluids are not representative, and a scaling method was not provided.

Pakzad et al. measured mixing times during agitation of a non-Newtonian fluid.[20, 21] They used a tank with diameter 40 cm, height 40 cm, and an impeller diameter of 18 cm. Their test fluid was xanthan gum solutions modeled as a Herschel-Bulkley fluid with a yield stress of 1.8 – 7.5 Pa. In their testing the mixing cavern included the entire vessel. They measured the mixing of an added conductive tracer throughout the vessel to determine the 95% of the steady state mixing time as a function of P/V (see Figure 4). The measured mixing time ranged from 15 – 60 seconds and for a given power per unit volume, the mixing times increase as the rheological properties increase. The data in Figure 4 show that as the rheology of the slurry increases, the mixing time increases or that increased power per unit volume is needed to achieve the same mixing time. From equation [1], the power per unit volume in the SRAT and SME is 12,400 W/m^3. The vessel in this testing was smaller than the SRAT and SME, and the power per unit volume was smaller, so caution should be used when applying these results to the SRAT and SME.

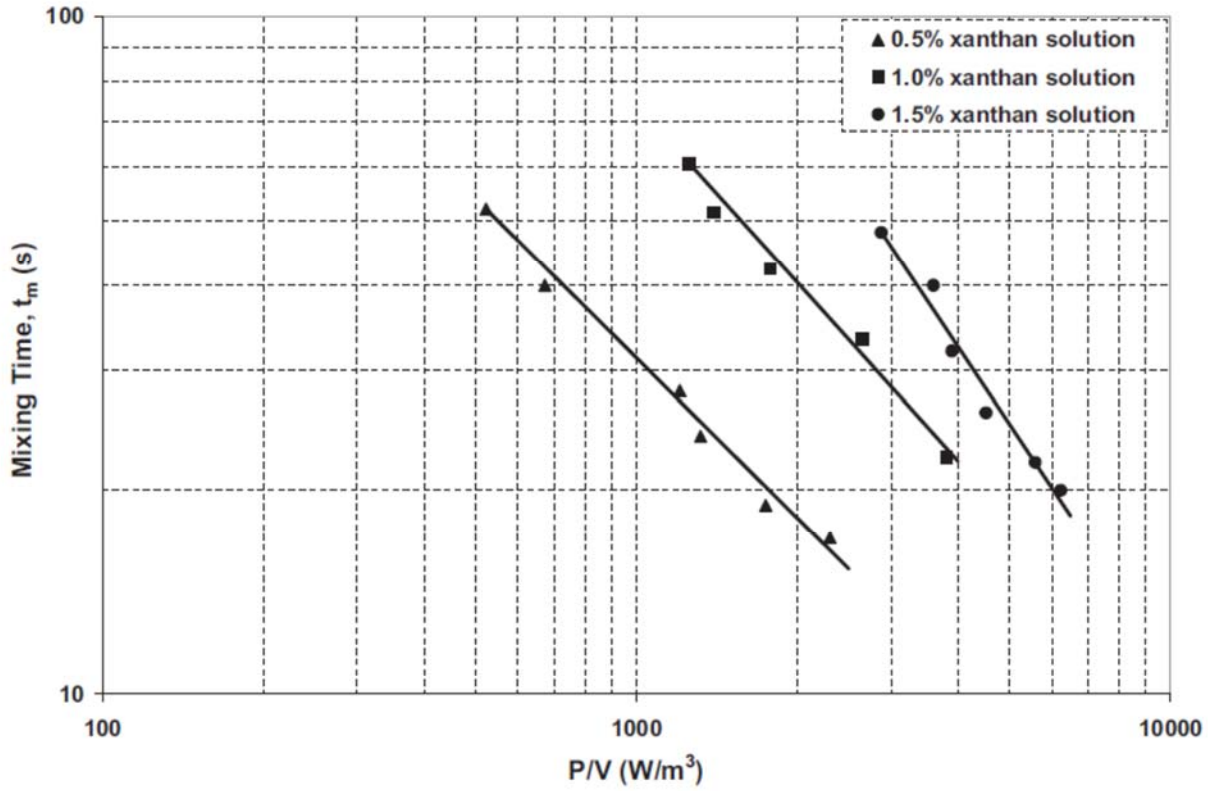

Figure 4 Measured Mixing Time with Xanthan Gum Solutions as a Function of Power Input[20]

Grenville measured the blend times of Newtonian and of pseudoplastic fluids.[22] The tank diameters were 0.3 – 1.8 m, baffled, and the Reynolds number was 200 – 100,000. The testing used pitched blade turbines, flat blade turbines, and hydrofoils (Lightnin A310 and Chemineer HE3) to mix the vessels. Blend time was measured by adding an electrolytic tracer to the vessel and measuring the change in conductivity at select locations in the vessel as a function of time. He found that the blend time ranged from 11 – 768 seconds and under turbulent conditions the pseudoplastic properties did not affect blending of the fluid.

Montante et al. measured mixing times of Newtonian and Pseudoplastic liquids in stirred tanks.[23] The work included CFD calculations and experiments. The vessels were tall cylindrical tanks of diameter 29 and 48 cm with multiple impellers on one shaft. The tank heights were 116 and 154 cm, a large H/D as compared to DWPF. The Reynolds number was 2500 – 10,000, turbulent. They found the tanks to be 95% blended in 10 – 75 seconds.

Adams and Barigou performed CFD calculations and measured the rate at which caverns and pseudocaverns (such are related to power law fluids) grew.[24] The tank diameters were 100 and 140 mm, with 4 equally spaced baffles, and the liquid height was equal to the tank diameter. The impeller was a 6-blade pitch blade turbine, diameter 1/3rd of the tank diameter, and located 1/3rd from the bottom of the tank. The Carbopol solutions had yield stresses of 1.3 – 2.6 Pa. A fluorescent dye was injected above the impeller, the mixer turned on at specific speeds, and the cavern growth monitored. The Reynolds numbers were 7.3 – 163 using effective viscosities based on applied agitator shear rate, and the time for the caverns to grow to 95% of their maximum size was 15 - 20 minutes, almost independent of the Re number, though the higher the Re the initial cavern growth was faster. The low Reynolds number in this work makes applicability of the results to the SRAT and SME of limited value.

CONCLUSION: The review of the technical literature describing the blending of Newtonian fluids and non-Newtonian fluids shows the mixing/blending to be a very fast process. In most instances the blend time was less than 2 minutes in small, pilot scale testing. The gas release time will be longer than the blend time, but the ratio of the two cannot be quantified. Investigating the blending time in the SRAT and SME is unlikely to provide the data needed to relax the assumptions on instantaneous release of hydrogen upon the start of agitation, and the focus of the investigation is on hydrogen release rather than mixing time. Therefore, no further investigation of blend time is recommended.

3.2 Quiescent Release

There are several forces acting on hydrogen bubbles while the SRAT and SME are quiescent. The forces include surface tension, hydrostatic pressure, buoyancy and viscous forces due in part from the rheological properties of the fluid. Before the bubbles will begin to move, the buoyancy force must exceed the viscous force due to the yield stress. Several works have measured or calculated a critical yield stress above which bubbles are stagnant, and below which bubbles will rise.[25,26,27,28,29,30]

Buoyancy forces scale with the volume of the bubble, while viscous forces scale with the surface area of the bubbles. Therefore, the bubble size required to overcome the viscous forces can be large. Equation [5] describes the balance of viscous (i.e., yield stress) and buoyancy forces

$$4\pi R_B^2 \tau_y = \frac{4}{3}\pi R_B^3 g \Delta\rho \cong \frac{4}{3}\pi R_B^3 g \rho_f \qquad [5]$$

where R_B is the gas bubble radius, τ_y is the slurry yield stress, g is gravitational acceleration, and $\Delta\rho$ is the density difference between the fluid/slurry and the gas bubble. The left side of equation [5] is the viscous forces ($4\pi R_B^2 \tau_y$), and the middle and right sides of equation [5] are the buoyancy forces ($\frac{4}{3}\pi R_B^3 g \Delta\rho$). The viscous force is calculated by multiplying the yield stress of the slurry by the surface area of the bubble, and the buoyancy force is calculated by multiplying the density difference between the bubble and the slurry by the gravitational constant and the volume of the bubble. Figure 5 shows a plot of the hydrogen bubble size (diameter) required to overcome the yield stress in a SRAT/SME slurry (assuming a hydrogen bubble density of 0.00009 g/cm^3 and a liquid density of 1.35 g/cm^3). With a yield stress of 1 Pa, the bubble diameter is greater than 450 μm, and with a yield stress of 10 Pa, the bubble diameter is greater than 4,500 μm.

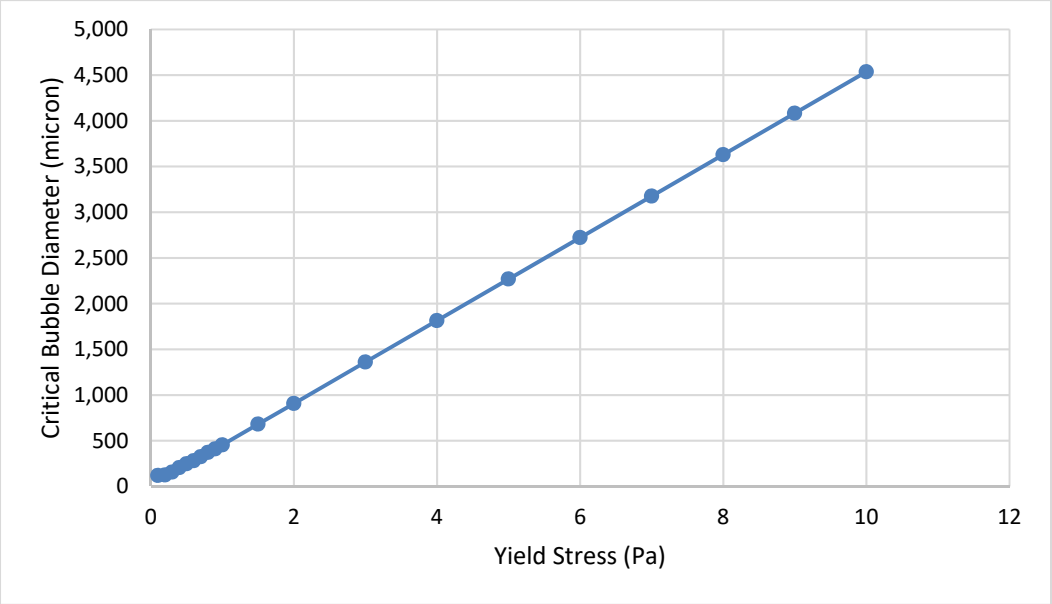

Figure 5. Critical Bubble Diameter to Overcome Yield Stress

Sikorski et al. investigated gas bubbles rising in a transparent yield stress fluid.[26] They correlated their data by plotting the Reynolds number of the rising bubbles against a yield parameter. The bubble Reynold number and yield parameter were defined by equations [6] and [7]

$$Re = \frac{2\rho v R_B}{\mu} \quad [6]$$

$$Y = \frac{2\pi\tau_y R_B^2}{\rho g V_b} \quad [7]$$

where ρ is the bubble density, v is the bubble rise velocity, R_B is the bubble radius, μ is the fluid viscosity, τ_y is the slurry yield stress, g is gravitational acceleration, and V_B is the bubble volume. The data shows the bubbles do not rise if Y is greater than 0.5. With a slurry yield stress of 1 Pa and a slurry density of 1.35 g/mL, the gas bubbles must be larger than 450 micron diameter to rise. If the yield stress is increased to 10 Pa, the gas bubbles must be larger than 4,500 micron diameter to rise.

Tsamopoulos et al. investigated bubble rise in Newtonian and viscoplastic fluids.[27] They used a Bingham number to correlate their data. Equation [8] defines the Bingham number.

$$Bn = \frac{\tau_y}{\rho g R_B} \quad [8]$$

They found for spherical bubbles to rise, the Bingham number was less than 0.143. Given a slurry with a yield stress of 1 Pa and density of 1.35 g/mL, the gas bubbles must be larger than 1060 micron diameter to rise. If the yield stress is increased to 10 Pa, the gas bubbles must be larger than 10,600 micron diameter to rise.

In addition to calculating a critical yield stress, some references calculated or measured a bubble rise velocity.[31,26,27,28] However, the data is graphical rather than analytical, so it is not useful in predicting bubble rise velocities for the SRAT/SME conditions. Given information of the bubble size, bubble concentration, vessel dimensions, settled solids volume, and rheology, this information could be used to calculate a

quiescent gas release rate. Unfortunately, the bubble size distribution and the properties of the settled slurry information is lacking for DWPF application and changing during the SRAT and SME cycles.

Some previous work found gas bubble retention to be a function of sludge depth.[32,33,34,35,36] However, none of these works describe the mechanisms for bubble retention being a function of depth. This finding is of importance, because it shows the scale of the vessel (i.e., height) could affect the quiescent release rate, and that not all hydrogen is retained.

During DWPF operation, if radiolysis is the primary means of hydrogen generation and the hydrogen generation from gamma radiation is significant, as the sludge settles, hydrogen may be formed in the supernate above the sludge. This hydrogen would not be retained.

Other works found the slurries to have a critical hold up volume (i.e., the maximum volume of gas that the sludge can retain), rather than retaining a specific fraction of the gas bubbles generated.[37,38,39,35] The data from the qualification of Sludge Batch 3 showed the hydrogen release rate to be less than the hydrogen generation rate in a quiescent vessel until a critical hold up volume was obtained. At that point, the hydrogen release rate equaled the hydrogen generation rate.[35] These results clearly indicate that saturation holdup exists, and additional generated gas is released. The vessels in this test were much smaller than the SRAT and the SME. The retention and release characteristics of the hydrogen and the sludge in those vessels are likely different.

Johnson et al. investigated the evolution of bubbles from yield stress fluids with a focus on the Sellafield and Hanford sites.[40] They had a tank diameter of 118 mm, a fluid volume of 1 L, and yield stresses of 4 – 234 Pa. The simulant was magnesium hydroxide powder blended with water. Gas generation was by use of hydrogen peroxide. Their data shows quiescent release of gas bubbles from slurries with yield stress that is similar to the contents of the SRAT (1.5 – 5 Pa) and SME (2.5 – 15). However, their vessel was smaller and the fluid height was less than the SRAT and SME, so caution should be used when applying these results to the DWPF. In this study, the bubble distribution for this range of yield stress reached a steady state condition with a maximum bubble diameter of 9000 microns, implying a dominant gas release mechanism dictated by the pore to millimeter scale bubble population, unrelated to the bubbles' buoyant force. Additionally, more than 50% of the generated gas was not retained. In addition, work described above showed that the fraction of gas retained increased with sludge depth, so the smaller volume and height could have led to less gas retention.

SRS measured hydrogen release in Tank 40, while the pumps were not running. The data showed measurable hydrogen release from a quiescent tank.[41,42] The author estimated the yield stress to be ~27 Pa, which is larger than the expected yield stress of the material currently in the SRAT and SME. Tank 40 is larger than the SRAT and SME and is mixed with slurry pumps rather than impellers. Tank 40 contained 41 inches of settled sludge and 59 inches of supernate. However, since the tank was quiescent during this release, the method of mixing should not be a factor, though the time frame of settling is significantly different. In addition, the tank contained a supernate layer above the settled sludge. This supernate would produce hydrogen from radiolysis and would have no yield stress. A fraction of the released hydrogen would be from radiolysis in the supernate. Whether this fraction is large or small is indeterminant from the documents. Given the difference in tank size, aspect ratio, settling time, and rheology, the quiescent release in the SRAT and SME would likely be different. Gas released during mixing was assumed to come from a combination of steady state generation, dissolved gas, and trapped gas.

During Slurry Run 1 in Tank 40, the purge rate was 175 ft^3/min, and the measured steady state hydrogen concentration was 7 ppm when the pumps were not running.[41] The tank diameter is 85 ft. Equation [9] calculates the quiescent release rate (Q).

$$Q = 0.000007 \frac{ft^3 H_2}{ft^3 Air} \cdot 175 \frac{ft^3 Air}{min} = 0.0012 \frac{ft^3 H_2}{min} \quad [9]$$

The cross-sectional area of the slurry-vapor interface is described by equation [10]

$$A = \frac{\pi}{4} D^2 = \frac{\pi}{4} (85 ft)^2 = 5675 ft^2 \quad [10]$$

Dividing the release rate by the cross-sectional area produces a release flux of 2.16 x 10^{-7} ft/min (1.30 x 10^{-5} ft/hr). Multiplying this quiescent release flux by the cross-sectional area of the SRAT (113 ft^2) produces a quiescent release rate in the DWPF SRAT of 0.011 gal/hr. At this release rate, the SRAT or SME would release 0.26 gallons of hydrogen per day. Tank 40 contains coiling coils which could slow the release of hydrogen gas under quiescent or agitated conditions. Under quiescent conditions, the coils would block the path of some of the bubbles to the slurry surface, and the coils would provide a surface to which the gas bubbles could attach. Under agitated conditions, the drag caused by the coils would reduce the momentum in the tank, which would reduce the agitation and rate of bubble release.

During another pump run in Tank 40, SRS measured hydrogen release with no slurry pumps operating. The quiescent release rate was 0.81 – 0.96 ft^3/hr.[42] Dividing the maximum release rate by the cross-sectional area of Tank 40 gives a release flux of 1.7 x 10^{-4} ft/hr. Multiplying this flux by the cross-sectional area of the SRAT, gives a quiescent release rate of 0.14 gal/hr. At this release rate, the SRAT and SME would release 3.4 gallons of hydrogen per day.

PNNL investigated gas retention in waste simulants using tall tanks.[43] The focus of their work was the waste tanks at the Hanford site. They conducted simulant testing in a column with a diameter of 60 inches and a sludge depth of 310 inches. The simulated settled sludge had a shear strength of 600 – 900 Pa. The simulant was a kaolin-water mixture containing iron micropowder, which corroded to produce hydrogen. The simulant contained enough iron to produce a 50 vol % hydrogen gas void fraction. The maximum gas void fraction observed was 8 – 12 vol %, and the gas fraction decreased after reaching a maximum. Their document suggests that significant quiescent release could occur with shear strengths much larger than expected in the SRAT and SME. However, PNNL characterizes their slurry by its shear strength. SRS typically characterizes slurries with a yield stress and consistency. The relationship between the two is complicated. For a quiescent slurry, the shear strength is the parameter that should be used.

Another PNNL work examined gas retention and release in clay simulants.[44] The testing was conducted in vessels with diameters of 12.7 cm and 58.4 cm. The simulants were a mixture of kaolin and finely ground silica in water. Gas was generated by the decomposition of hydrogen peroxide (oxygen generator) or corrosion of iron (hydrogen). The simulant shear strength ranged from 15 – 1800 Pa. The results showed a difference in the shape of retained bubbles when using hydrogen peroxide and iron, and the rate at which the gas was produced. The results suggested a difference in retention between oxygen and hydrogen. A lower peak gas retention was observed when gas was generated from iron particles (12.7 vol %) as compared to hydrogen peroxide (19 vol %). Plausible reasons for the difference include the smaller size of hydrogen gas molecules, the lower molecular weight of the hydrogen gas molecules, or the higher molecular diffusivity of the hydrogen. This difference should be considered when applying gas retention data using oxygen to the SRAT and SME.

CONCLUSION: The literature on gas release from quiescent yield stress fluids indicates that large sized gas bubbles (500 – 4,500 micron) would be needed to overcome the yield stress via buoyant forces and rise to the surface in SRAT and SME type slurries. Data from the DWPF, the SRS Tank Farm, and the SRNL Shielded Cells showed hydrogen gas release from a quiescent slurry of SRS sludge. Testing at the University of Leeds shows quiescent release of gas bubbles from slurries that had yield stresses similar to the contents of the SRAT and SME with bubble buoyance not dictating bubble size.[40] Testing by PNNL

with a tall column found the amount of hydrogen retained to be much smaller than the amount generated.[43] Work at SRS showed the fraction of hydrogen retained varied with sludge depth. These results show that gas can be released from a yield stress fluid under quiescent conditions, and additional work should be performed to attempt to relax the assumption that all hydrogen gas generated in the SRAT and SME is retained. In performing this work and assessing the results, slurry shear strength should be used to describe the slurry rheology.

3.3 Agitated Release

3.3.1 DWPF Operating Experience

Bodey examined DWPF facility data from the SRAT that included Sludge Batches 5, 6, 7a, 7b, and 8 and compared the facility measured hydrogen gas concentration with the lower flammability limit.[45] The evaluation reviewed 158 potential hydrogen gas release events in the SRAT. It identified a limited number of events where a small hydrogen release was detected upon agitator restart. The size of the hydrogen release was smaller than would be expected even if only a moderate fraction of the hydrogen generated was retained within the sludge. These observations suggest that a significant fraction of the hydrogen generated under quiescent conditions was released. However, the document does not quantify the amount released or the release rate under quiescent conditions.

Table 1 shows the catalytic hydrogen generation rates in previous sludge batches based on a 6,000 gallon slurry volume. The table shows significant differences in the hydrogen generation rate in Sludge Batches 5, 6, and 7a compared with Sludge Batches 7b and 8. This data is included for completeness, but it will not be used for analysis or calculations. If future sludge batches have higher hydrogen generation rates, understanding the amount of hydrogen retained under quiescent conditions and the rate at which hydrogen is released upon the start of agitator operation will be important for the DWPF. An effort should be started to review the hydrogen release data during processing of these sludge batches to attempt to quantify the quiescent release rate and the release rate upon the start of agitation in the SRAT and SME.

Table 1. Characteristic Hydrogen Generation Rates of the DWPF Sludge Batches

Sludge Batch (SB)	Beginning Dates	Catalytic Hydrogen Generation Rate[lb_m/hr]
SB5 Receipt	December 2008	0.495
SB5 Product		
SB6 Receipt	June 2010	0.55
SB6 Product		
SB7a Receipt	June 2011	0.24
SB7a Product		
SB7b Receipt	January 2012	0.014
SB7b Product		
SB8 Receipt	May 2013	0.028
SB8 Product		

3.3.2 Sludge Batch Qualification

SRNL conducted demonstrations of the SRAT and SME cycles with actual waste as part of the qualification for Sludge Batches 6, 7a, and 7b.[46,47,48] The testing included rheology measurements shown in Table 2. The rheology varied throughout the testing, and in some cases exceeded the design limits for the DWPF. The demonstrations included simulating the SRAT cycle and the SME cycle in the DWPF. The SRAT cycle included concentration by boiling to raise the insoluble solids concentration, cooling for sampling, heating, addition of nitric and formic acids, concentration to remove water by boiling, and reflux to achieve a target boiling time. The SME cycle included addition and removal of water, addition of frit and dilute formic acid, and concentration by boiling to achieve a target total solids concentration. As part of the testing, they measured the rate of gas release during agitation. During these tests, they observed the hydrogen release to occur over several hours, rather than instantaneously. However, the hydrogen was generated over several hours rather than instantaneously. In addition to mixing the vessel with impellers, the contents of the vessel were boiling, which increased transport of hydrogen to the slurry-vapor interface and increased the rate of hydrogen release. This data is not useful in assessing the relaxation of the conservative assumptions in the hydrogen retention program.

Table 2. Rheology of Sludge during Batch Qualification Testing

Batch	Yield Stress (Pa)	Consistency (cP)
SB5	**1.5 – 16.7**	**6.1 – 14.3**
SB6	**8.3 – 21**	**8.9 – 15**
SB7a	**1.8 – 8.1**	**7.3 – 10**
SB7b	**4 - 21**	**10.6 – 38.1**

In some of the SRNL tests for waste feed qualification of a sludge batch, hydrogen release was observed as the SRAT/SME demonstration testing started.[49,50,46] This measured hydrogen is believed to be retained hydrogen released upon the start of agitation and heating of the SRAT feed material. The release is believed to represent a release upon the start of mixing, but the head space volume and time to reach the detector spread the peak over a period of time, which complicates determining the exact timing of the release and determination of the release rate. In these tests, the slurry volume was ~ 1 Liter, the head space was ~ 500 mL, and the air purge rate was ~ 370 standard cm^3/min.[d]

With the qualification of Sludge Batch 3, 50% of the "retained hydrogen" was released over ~22 minutes (see Figure 6).[35] With Sludge Batch 5 qualification, 50% of the "retained hydrogen" was released over ~45 minutes (see Figure 7).[51]

[d] For the Sludge Batch 3 qualification testing, the sludge volume was approximately 342 mL, the head space volume was approximately 1158 mL, and the air purge was approximately 98 cm^3/min.

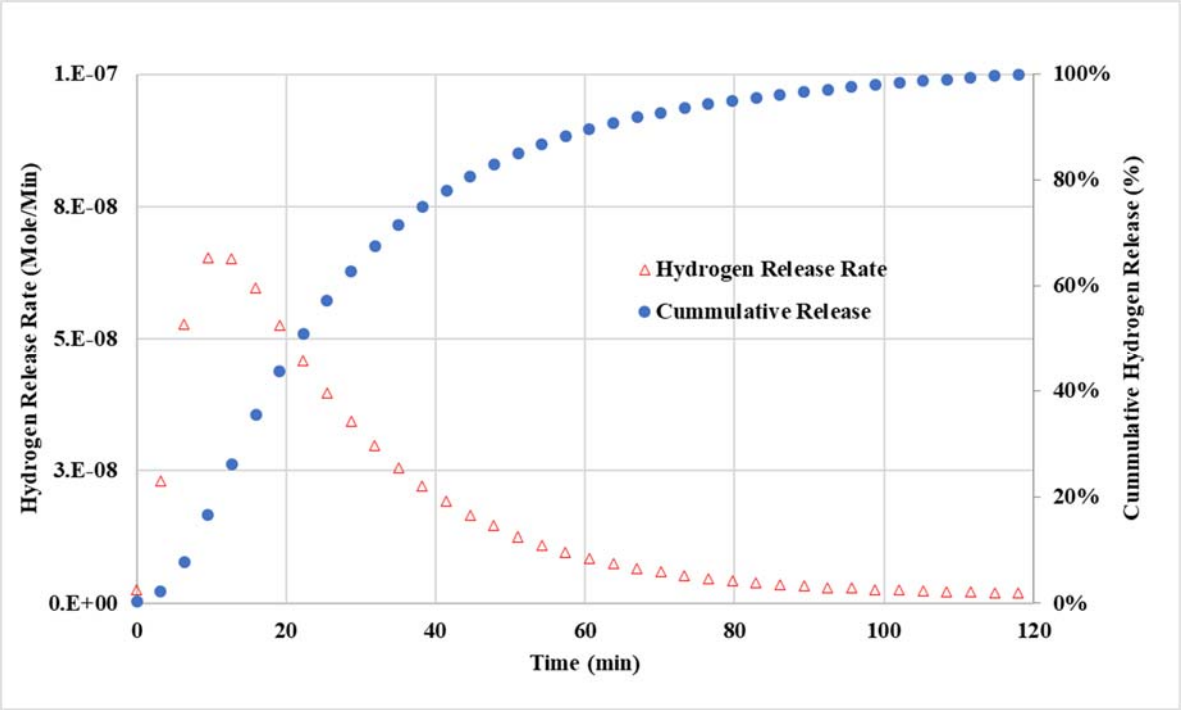

Figure 6. Retained Hydrogen Release at the Start of Mixing in Sludge Batch 3 Qualification

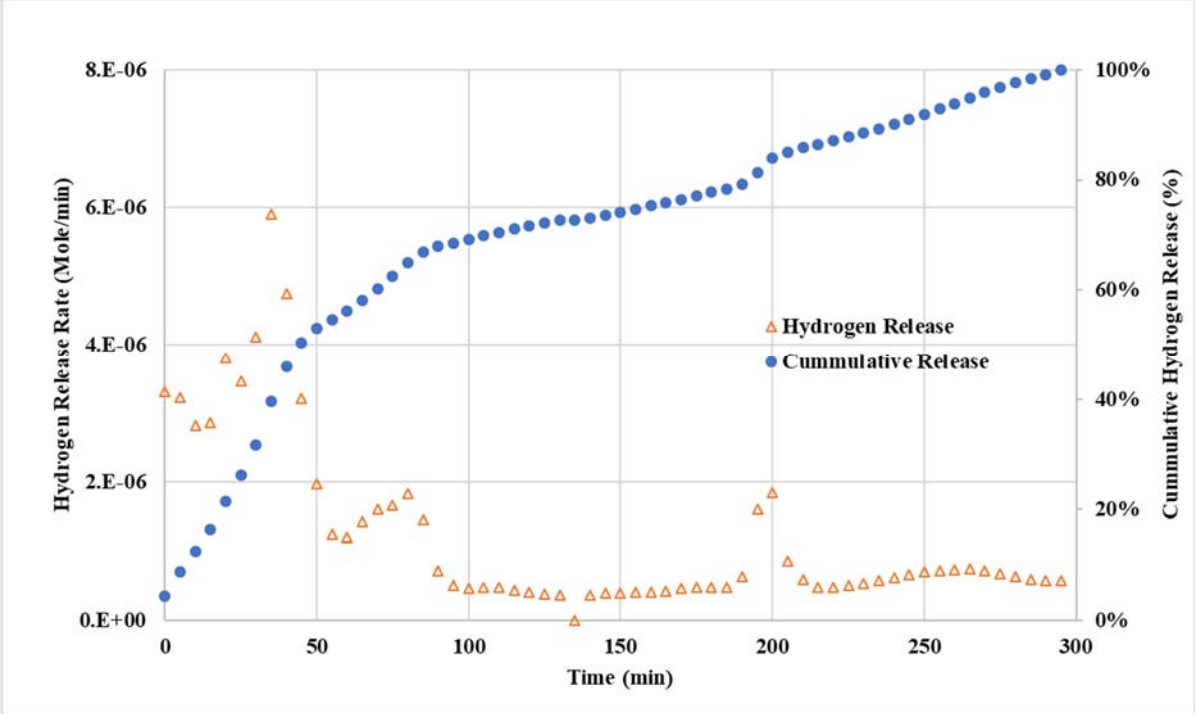

Figure 7. Retained Hydrogen Release at the Start of Mixing in Sludge Batch 5 Qualification

The "retained" hydrogen release data from Sludge Batch 3 between 16 and 83 minutes was fit with an exponential decay mode that assumes the hydrogen was released instantaneously upon the start of agitation.

The model curve fitted the data from 16 minutes to 83 minutes using Excel and the results shown in Figure 8 as "data fit".

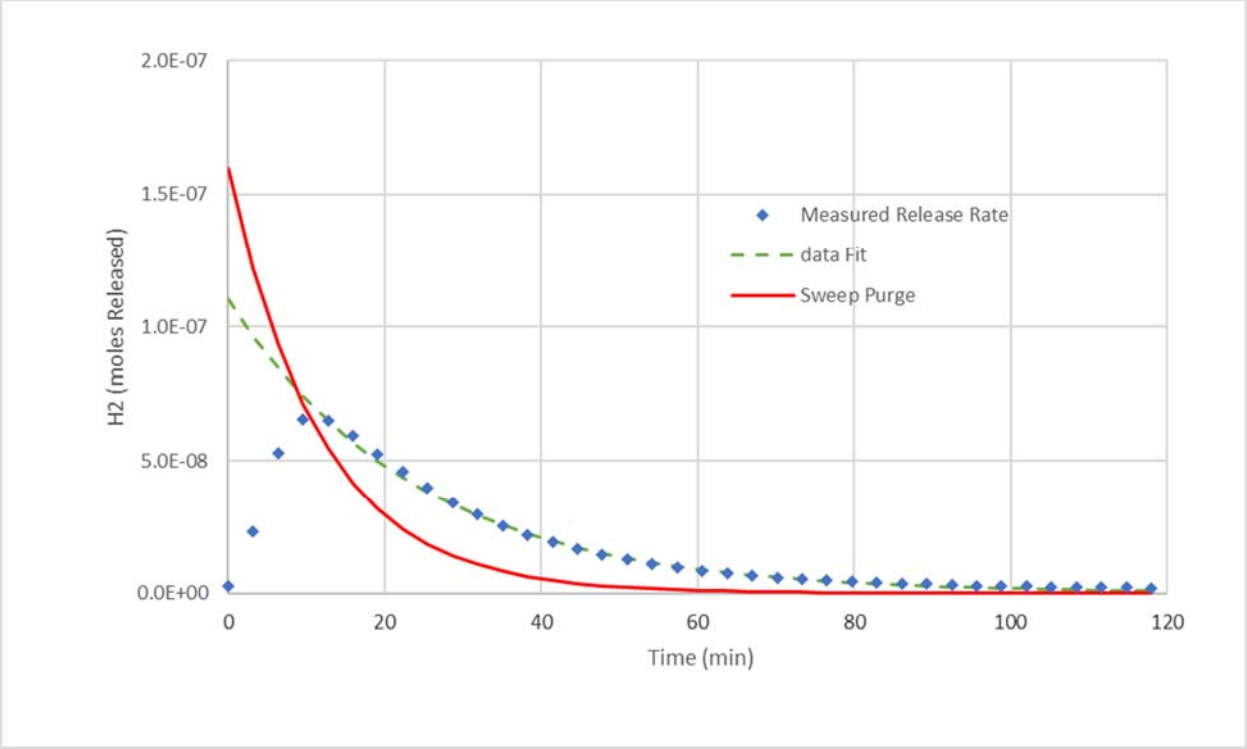

Figure 8. Analysis of Instantaneous Retained Hydrogen Release at the Start of Mixing in Sludge Batch 3 Qualification

The DWPF hydrogen retention program assumes that all the retained hydrogen is released instantaneously when agitation starts.[52] A calculation was performed to predict the hydrogen concentration as a function of time from an instantaneous hydrogen release. The hydrogen concentration as a function of time from a purge of the head space is described by equation [11]

$$C(t) = C_o e^{-\frac{QKt}{V}} \qquad [11]$$

where C_0 is the initial concentration in the head space, Q is the purge rate of the head space (98 SCCM from SB3 qualification), K is the mixing efficiency factor (assumed to be 1 for perfect mixing), t is time, and V is the head space volume (1158 cm^3 from SB3 qualification).[53] For the calculation, C_0 was selected to have the same amount of hydrogen release as measured during the sludge batch qualification. This calculation, Sweep Purge, is included in Figure 8. Comparing the predictions of the hydrogen concentration in the head space based on an instantaneous release and a sweep purge of the head space with the measured hydrogen concentration shows that the release of the "retained" hydrogen was not instantaneous. This phenomenon should be further investigated with testing and computational fluid dynamics modeling.

The SB3 qualification vessel was 10 cm in inner diameter and contained ~ 342 mL of sludge. It was mixed with a 2-inch diameter flat blade turbine (N_p= 4). The impellers impeller speed was not provided in the document. Assuming a fluid density of 1.27 g/mL and an impeller speed of 250 rpm, the power per unit volume was 1245 g/cm sec^3, which is significantly less than the SRAT. Given the P/V for the SRAT/SME is much larger (equation [1]) than the SB3 qualification run, the release rate in the SRAT/SME would likely be faster. In addition, the DWPF SRAT and SME operate under turbulent

mixing conditions, while the vessel used for the batch qualification testing had a much lower Reynolds number (1400 with a consistency of 10 cP and an impeller speed of 250 rpm) and may have operated under transition or laminar flow conditions.

3.3.3 Tank 51 Operating Experience

SRS personnel measured hydrogen release during slurry pump operation in Tank 51.[54] They observed the hydrogen release to occur over 52 hours. The peak hydrogen concentration in the vapor space was observed approximately 2 hours after the start of the third slurry pump. Approximately 20% of the released hydrogen was released in the first two hours. Approximately 7 hours after the start of the third pump, a power outage stopped all the slurry pumps. The vessel continued to release hydrogen.

There are a couple of factors that could affect the hydrogen release rate and measured hydrogen concentration in the purge gas that need considered. These factors include the mixing time and the ratio of the head space volume to the purge rate. The paper provides measured data on the sludge height under select risers (E1, B3, and C3) as a function of time. The measured sludge height below riser E1, which is 5.8 meters from the center of the slurry pump in riser B1, decreased from 184 cm to 3 cm within one hour. The measured sludge height below riser B3, which is 6.9 meters from the center of the slurry pump in riser B4, decreased from 195 cm to 92 cm in one hour. The measured sludge height below riser C3, which is 7.5 meters from the center of the slurry pump in riser H, decreased from 194 cm to 47 cm in one hour. These data show that the time to mix and suspend the sludge, was at least one hour, and it could be several hours. This mixing time for the sludge that released hydrogen could have contributed to the extended to the extended time over which the release occurred.

Tank 51 contained a sludge height of 191 cm (264,000 gallons). The height of the tank is 10 m, so it has a volume of 1,382,000 gallons. Subtracting the volume of sludge gives a head space of 1,118,000 gallons.[e] With a purge rate of 8500 liters per minute, the turnover time of the head space is 8.3 hours. This turnover time would make any rapid release of hydrogen appear to occur over a longer time. Tank 51 was mixed with rotating slurry pumps rather than impellers.

The slurry pumps will produce a horizontal flow, which will have a different flow pattern than that produced by the impellers and draft tube in the SRAT and SME. Quantifying the impact of this difference is difficult. Differences in power input and vessel volume can be estimated by comparing the power per unit volume in Tank 51 with the SRAT and SME.

Three quad volute slurry pumps were operating at 1500 rpm (1020 gpm per 3-inch nozzle).[f] The mean measured cleaning radius of the pumps was 6.6 m when operating at 2200 rpm, so using the pump affinity laws and assuming the cleaning radius is proportional to the pump speed, the expected cleaning radius is 4.5 m. The height of the fluid was 1.95 m. Assuming a fluid density of 1.35g/mL, and treating the mixed region as a cylinder (from rotation of the pumps) with diameter 6.6 m and height of 1.95 m, the power per unit volume was calculated with equations [12], [13], and [14].

$$P = \frac{\pi}{8}\rho D_j^2 V_j^3 = \frac{\pi}{8}\left(1.35\frac{g}{cm^3}\right)(7.62cm)^2\left(1414\frac{cm}{s}\right)^3 = 8.7\ x\ 10^{10}\frac{g\ cm^2}{s^3} \quad [12]$$

$$= 1.7\ x\ 10^{11}\frac{g cm^2}{s^3} \text{for two nozzles}$$

[e] The actual head space volume is likely less, but no volume is given for the supernate in the tank. The supernate volume is assumed to be 0 for this calculation. Including the supernate volume would reduce the head space volume and the turnover time for the head space.

[f] One of the pumps was initially operating at 1900 rpm, but its speed was reduced to 1500 rpm due to increasing hydrogen concentration. 1500 rpm was used for the calculations.

$$V = \pi HR^2 = 1.24\ x\ 10^8 cm^3 \quad [13]$$

$$\frac{P}{V} = 1370 \frac{g}{cm\ s^3} \quad [14]$$

where D_j is the jet nozzle diameter, V_j is the nozzle discharge velocity, R is the cleaning radius of the pump, and H is the fluid height in the vessel.[55] The applied power per unit volume in Tank 51 is much less than in the DWPF SRAT.

3.3.4 Tank 40 and 8 Operating Experience

Hester reported measured hydrogen release rates during the operation of slurry pumps in Tanks 40 and 8.[41,42] The investigation found that after the start of the pumps, the hydrogen release occurred over several hours, rather than instantaneously. This analysis will look at data from Runs 1 and 3 of Tank 40, because those runs showed the highest concentrations of hydrogen in the vapor space and the initial release occurred over approximately 2 days. The level of the sludge plus the supernate was 100 inches, and the height of the tank was 396 inches giving a head space height of 296 inches, or 1,039,000 gallons. The purge rate was 175 SCFM or 1309 gpm. Dividing the head space volume by the purge rate gives a turnover time for the head space of ~ 13 hours. This turnover time is likely a contributor to the long release time observed, but it may not be the only cause. The analysis will also look at Run 2 in Tank 8. The initial release from Slurry Pump Run 2 in Tank 8 occurred over approximately 2 days. The level of the sludge plus the supernate was 75 inches, and the height of the tank was 396 inches giving a head space height of 321 inches, or 1,127,000 gallons. The purge rate was 730 SCFM or 5460 gpm. Dividing the head space volume by the purge rate gives a turnover time for the head space of ~ 3.4 hours. This turnover time is likely not the primary contributor to the long release time observed, but it may be a secondary contributor. The mixing time to suspend the sludge and transport the hydrogen to the liquid surface could also be a contributor to the extended release time. Unfortunately, the documents do not provide any information that could be used to determine the mixing time in these tanks.

During Run 1 in Tank 40, one quad volute slurry pump was operating at 1800 rpm (1227 gpm per 3 inch nozzle) during the maximum release. Based on a yield stress of 27 Pa, density of 1.35 g/cm^3, the calculated cleaning radius is 29 ft using Churntski's equation.[56] Accounting for the influence of cooling coils, this cleaning radius is revised to 15 ft based on testing conducted to evaluate the impact of cooling coils on liquid blending.[57] The height of the sludge was 41 inches and the height of the supernate was 59 inches (100 inches total). Assuming a fluid density of 1.35g/mL, and treating the mixed region as a cylinder with radius 15 ft and height of 100 inches, the power per unit volume was calculated with equations [15], [16], and [17].

$$P = \frac{\pi}{8}\rho D_j^2 V_j^3 = \frac{\pi}{8}\left(1.35 \frac{g}{cm^3}\right)(7.62cm)^2 \left(1707 \frac{cm}{s}\right)^3 = 1.53\ x\ 10^{11} \frac{g\ cm^2}{s^3} \quad [15]$$

$3.06\ x\ 10^{11} \frac{g\ cm^2}{s^3}$ for two nozzles

$$V = \pi HR^2 = 1.67\ x\ 10^8 cm^8 \quad [16]$$

$$\frac{P}{V} = 1836 \frac{g}{cm\ s^3}^3 \quad [17]$$

The applied power per unit volume for Run 1 in Tank 40 is less than in the DWPF SRAT, similar to the Tank 51 operations.

During Run 3 in Tank 40, one quad volute slurry pump was operating at 1650 rpm (1125 gpm per 3 inch nozzle) during the maximum release. Based on a yield stress of 27 Pa and slurry density of 1.35 g/cm^3, the calculated cleaning radius is 27 ft. Accounting for the influence of cooling coils, this cleaning radius is revised to 14 ft. The height of the sludge was 41 inches and the height of the supernate was 59 inches (100 inches total). Assuming a fluid density of 1.35g/mL and treating the mixed region as a cylinder with

diameter 14 ft and height of 100 inches, the power per unit volume was calculated with equations [18], [19], and [20].

$$P = \frac{\pi}{8}\rho D_j^2 V_j^3 = \frac{\pi}{8}\left(1.35\frac{g}{cm^3}\right)(7.62cm)^2\left(1550\frac{cm}{s}\right)^3 = 1.15\ x\ 10^{11}\frac{g\ cm^2}{s^3} \quad [18]$$

$2.29\ x\ 10^{11}\frac{g\ cm^2}{s^3}$ for two nozzles

$$V = \pi HR^2 = 1.45\ x\ 10^8 cm^3 \quad [19]$$

$$\frac{P}{V} = 1598\frac{g}{cm\ s^3} \quad [20]$$

The applied power per unit volume for Run 3 in Tank 40 is less than in the DWPF SRAT.

The headspace during the demonstration in Tank 40 was approximately 1,039,000 gallons, and the purge rate was 175 SCFM. The turnover time of the headspace was ~ 13 hours. This long turnover time would have reduced the maximum measured hydrogen concentration in the purge and extended the duration of the measured hydrogen release. Because of differences in vessel size, mixing equipment, power input, head space volume, and purge rate, caution should be used in applying these results directly to the SRAT and SME.

During Tank 8 Run 2, one standard slurry pump was operating at 600 rpm (200 gpm per 1.5-inch nozzle) during the maximum release. Based on a yield stress of 200 Pa and slurry density of 1.35 g/cm^3, the calculated cleaning radius is 3.5 ft. Because of the small calculated cleaning radius, no correction was made for the cooling coils. The height of the sludge was 43 inches and the height of the supernate was 32 inches (75 inches total). Assuming a fluid density of 1.35g/mL and treating the mixed region as a cylinder with radius 3.5 ft and height of 75 inches, the power per unit volume was calculated with equations [21], [22], and [23].

$$P = \frac{\pi}{8}\rho D_j^2 V_j^3 = \frac{\pi}{8}\left(1.35\frac{g}{cm^3}\right)(3.81cm)^2\left(1100\frac{cm}{s}\right)^3 = 1.02\ x\ 10^{10}\frac{g\ cm^2}{s^3} \quad [21]$$

$2.04\ x\ 10^{10}\frac{g\ cm^2}{s^3}$ for two nozzles

$$V = \pi HR^2 = 6.81\ x\ 10^6 cm^3 \quad [22]$$

$$\frac{P}{V} = 3008\frac{g}{cm\ s^3} \quad [23]$$

The applied power per unit volume in Tank 8 is similar to the DWPF SRAT.

The headspace during the demonstration in Tank 8 was approximately 1,127,000 gallons, and the purge rate was 730 SCFM. The turnover time of the headspace was ~ 3.4 hours. This long turnover time would have reduced the maximum measured hydrogen concentration in the purge and extended the duration of the measured hydrogen release. Because of differences in vessel size, mixing equipment, power input, head space volume, and purge rate, caution should be used in applying these results directly to the SRAT and SME.

3.3.5 Florida International University Testing

Patel et al. performed gas retention and release experiments with low yield stress kaolin/bentonite slurries.[58] The gas, oxygen, was generated in situ via the decomposition of H_2O_2. The vessel was 6 ft tall, 6" diameter, and contained three impellers and a lower rake impeller to better mobilize the lower section of the vessel. In these tests, the slurry sat quiescent for 18 hours before release. When agitation started, the initial, constant release occurred over 5 – 15 minutes, with peak concentrations occurring in the initial 2-3 minutes. Following the initial release, a slower, steady release occurred over the next 100 minutes. The L/D of these

tests was very high and could limit the applicability to the SRAT/SME vessels. Release rates were inversely proportional to bulk yield stress of the clay mixtures utilized.

CONCLUSION: Data from SRNL DWPF Batch Qualification testing showed the release of retained hydrogen occurred over several minutes rather than instantaneously. Data from the SRS Tank Farm during pump mixing showed the hydrogen release to occur over several hours rather than instantaneously. Simulant testing conducted at Florida International University showed the release of retained gas occurred over several minutes rather than instantaneously. Because of differences in agitation intensity, agitation method, vessel volume, headspace volume, purge rate, and power input, this data cannot be directly applied to the DWPF. Nevertheless, the combined data provides confidence that a release rate slower than instantaneous is valid for the SRAT and SME vessels. Additional work is recommended to quantify the applicable release rates.

3.4 Changes in Rheology

The ability to retain hydrogen has been shown by PNNL to be a function of the settled solids shear strength (not the Bingham Plastic yield stress, which is obtained from a flow curve) as shown in Figure 9.[59] The mechanism for gas release changes as the settled solids shear strength increases as shown in Figure 9. For low shear strength material, less than 10 to 20 Pa, bubbles can escape as individual bubbles and retention in the settled sludge can be as great as 20% by volume. As the settled solids shear stress increases between 20 to 200 Pa, gas retention increases to 40% by volume. In this region, the quantity of gas released increases with larger fractions of the retained gas prior to retaining newly generated gas, where this cycles between a minimum and maximum as the additional gas is generated and then released. Above 200 Pa settled solids shear strength, the volume of retained gas decreases as the settled solids shear strength increases. Once the maximum settled solids shear stress is obtained, the generated gas is released continuously at the rate it is generated by following paths (fissures) in the settled solids. Figure 9 cannot be used to determine how much gas can be retained for SRS sludges, but does show different mechanisms that could exist for SRS sludge and these depend on the settled solids shear strength.

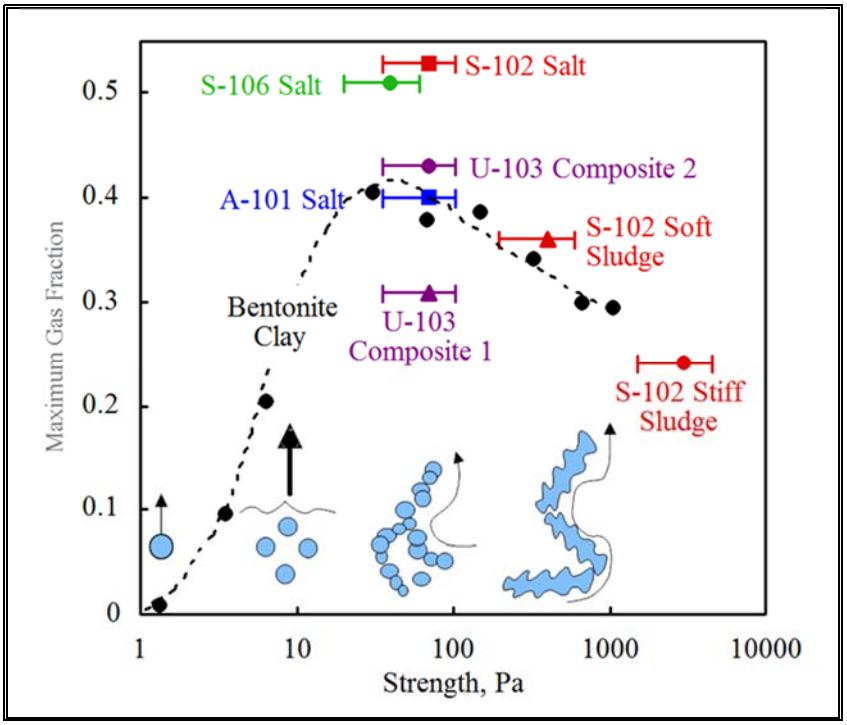

Figure 9. Effects of Waste Strength on Gas Retention and Natural Release Mechanisms

SRNL and PNNL have performed studies on radioactive sludge, where both flow curves (to obtain Bingham Plastic fluid parameters) and settled solids shear strength (using the vane method)[60,61] have been measured on the same sludge, given a starting weight percent total or insoluble solids.[62,63,64,65] Gas retention was not measured during these activities, vane measurements were obtained from a single level, and none of the sludges were SRS sludges. Additionally, understanding of how starting wt % solids impact settled solids shear strength is limited. The results from these studies are summarized in Table 3, which clearly shows that the settled solids shear strength in general is greater than the Bingham Plastic yield stress and at times, much greater within a 24 hour period. Simulant testing has also supported this position. The AZ-101 sludge showed the settled solids shear stress increase by a factor of three and then levels off after 5 days of testing.

Table 3. Bingham Plastic and Settled Solids Shear Strength Properties of Radioactive Waste

Sludge/Tank	wt % Total Solids	wt % Insoluble Solids	Yield Stress (Pa)					
			Bingham Plastic	Settled Solids Shear Strength as a function of settling time (hr)				
				0	9	24	48	65
AY102/C106	20.4	-	1.6	0	14.1	4.2	-	-
	27.1	-	12	20.4	23.5	20.2	-	32.7
MVST-24	-	27.22	22.8	-	-	58	-	-
MVST-25	-	17.78	3.5	-	-	9.3	-	-
MVST-28	-	16.23	19.1	-	-	72	-	-
MVST-30	-	29.65	33	-	-	130	-	-
AZ-101	-	22	11.4	See Figure 10				
T-204	18	-	3	-	-	-	20	-
B-203	28.6	-	10.9	-	-	-	60	-
T-203	30.7	-	38.6	-	-	-	310	-

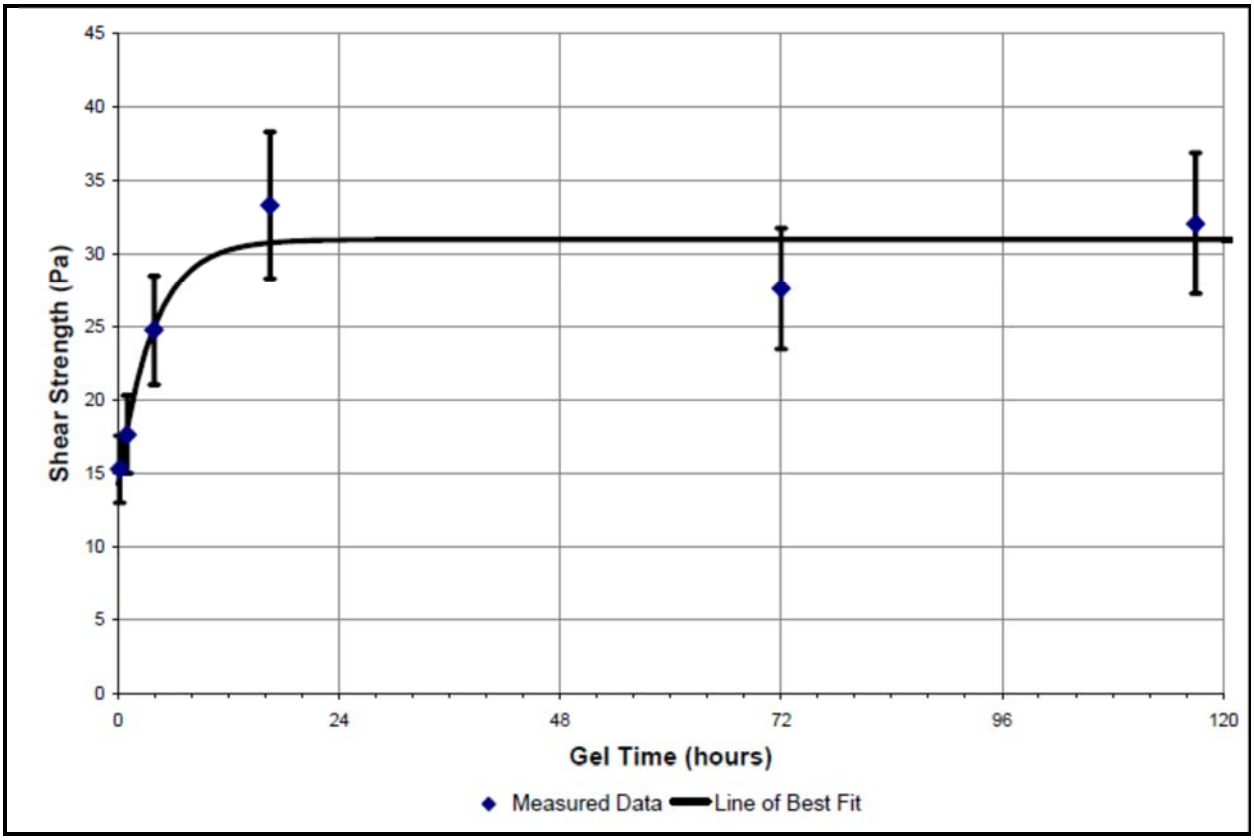

Figure 10. AZ-101 Settled Solids Shear Stress Versus Settling Time

Additional testing is recommended with actual waste to better understand how quiescent conditions and depth in the SRAT and SME will change slurry rheology and its impact on gas retention and release. These efforts would be integrated, and a method could be developed to assess the impact of settled solids shear stress (shear strength) on retention and release.

CONCLUSION: Previous work by SRNL and PNNL has measured the rheology of Hanford sludge, and shown the rheology to increase as the sludge is allowed to settle. Potential changes in sludge rheology need considered when assessing changes to the DWPF retained hydrogen program.

4.0 Preliminary Calculations

Two calculations were performed to support the data obtained in the literature search (Section 3). The first calculation was to compare the momentum from droplets rising due to buoyancy with the momentum of the fluid motion in the SRAT and SME. The second calculation was a preliminary Lattice-Boltzmann computational fluid dynamics (CFD) calculation performed on a simple SRAT type mixing configuration. These calculations are described below.

4.1 Bubble Motion in a Stirred Tank

As gas bubbles form and the SRAT vessel is mixed, a number of forces act on the bubbles. These forces include inertia from the slurry fluid motion, buoyancy from the difference in density between the gas bubble and the slurry, surface tension, pressure, and viscous forces. Two forces that will have the most impact on whether the gas bubbles reach the surface are buoyancy and inertia. This section will compare the buoyancy and inertia forces acting on the bubbles.

To compare these forces, a representative bubble size must be selected. Machon et al. developed a correlation to predict bubble size in an agitated vessel.[66] The correlation is described by equation [24]

$$d_{32} = 2.25 \frac{\sigma^{0.6}}{(P/V)^{0.4}\rho^{0.2}} \epsilon_H^{0.4} \left[\frac{\mu_G}{\mu_L}\right]^{0.25} \quad [24]$$

where d_{32} is the Sauter mean diameter of the bubble, σ is the surface tension of the bubble, P/V is the applied power per unit volume, ρ is the fluid density, ε_H is the gas hold up fraction, μ_G, is the gas viscosity, and μ_L is the liquid viscosity. The following values were selected for the parameters in equation [24]:

σ = 71 x 10^{-3} N/m

ρ = 1380 kg/m^3

ε_H = 0.05

P/V = 12,400 g/cm s^3 = 1,240 kg/m s^3

μ_G = 0.88 x 10^{-5} Pa s

μ_L = 12 x 10^{-3} Pa s

The surface tension selected is the surface tension for helium in water. Review of the literature shows the surface tensions of helium, nitrogen, and air with water are approximately the same. Helium was selected, because its molecular weight is the closest to hydrogen.[67] A density of 1380 kg/m^3 was selected based on the as received slurry density for Sludge Batch 6 qualification.[46] A gas hold up fraction of 0.05 was assumed for the calculation.[g] The power per unit volume of the SRAT was calculated previously. The hydrogen viscosity is from the International Critical Tables and is the viscosity at 23˚C.[68] The liquid viscosity was selected as the maximum consistency expected in the SRAT.[1] Using these values, the calculated mean bubble diameter is 311 μm. Using this bubble diameter and a bubble density of 0.083 g/L based on the density of hydrogen gas at 20˚C, calculated using the ideal gas law, the bubble rise velocity can be calculated with Stokes Law using equation [25]

$$V_{rise} = \frac{gd^2(\rho_f - \rho_g)}{18\mu_L} = \frac{980\frac{cm}{s^2}(0.031cm)^2(1.38-0.000083)\frac{g}{cm^3}}{18\left(0.12\frac{g}{cm\,s}\right)} = 0.60\frac{cm}{s} \quad [25]$$

Multiplying the rise velocity by the bubble density yields a bubble rise momentum of 0.00005 g/(cm^2 s).

The fluid velocity was calculated by assuming the fluid motion is downward inside the draft tube formed by the cooling coils and upward outside of the draft tube formed by the cooling coils. The flow rate was calculated with equation [26].

$$Q = N_Q N D^3 = 0.7\left(\frac{130}{60}rps\right)\left(3ft\frac{30.48cm}{ft}\right)^3 = 1.16\,x\,10^6\ \frac{cm^3}{s} \quad [26]$$

The flow number (N_Q) in equation [26] is for a flat blade turbine (N_Q= 0.7).[2] The axial flow impeller in the SRAT and SME may increase the flow but was not used in the calculation for conservatism. The flow rate is divided by the annular area on the outside of the cooling coils to calculate a fluid velocity in equation [27]

$$A = \frac{\pi}{4}\left(D_o^2 - D_i^2\right) = \frac{\pi}{4}\left((12ft)^2 - (5ft)^2\right)\left(\frac{30.48cm}{ft}\right)^2 = 87{,}000cm^2 \quad [27]$$

[g] The gas holdup fraction is the fraction of the slurry volume that is composed of gas rather than liquid or solid particles. It is different from the fraction of generated hydrogen that is retained in the slurry.

Using the results from equation [26] and [27], the calculated fluid velocity is 13.3 cm/s. Multiplying by the fluid density, the momentum is 18 g/(cm^2 s), which is more than 350,000X the momentum calculated from buoyancy.

The momentum of the fluid motion from the impellers is much larger than the momentum from the bubbles rising, so the bubbles will follow the fluid motion and only be released if the fluid motion causes them to reach the surface.

4.2 MSTAR CFD Calculation

MSTAR CFD is a Lattice Boltzmann computation fluid dynamics program that can describe multiphase physics and chemical processes. As part of this exploration, SRNL requested that the vendor perform a calculation on a SRAT type vessel. The vessel diameter was 12 ft diameter, the vessel height was 16.5 ft, and the liquid level was 10.5 ft. The vessel was mixed with a 4-blade flat blade impeller and a 3-blade propeller placed at locations to represent the SRAT. The impellers rotated at 100 rpm. The liquid density was 1 g/mL and the liquid viscosity was 20 cP. After reaching steady-state, 150,000 gas bubbles of 1 mm diameter were added to the vessel. (The diameter was selected arbitrarily and does not necessarily reflect the value representative of the DWPF application.) Approximately 50% of the bubbles released to the vapor space over ~80 seconds. The simulation showed the bubbles to follow the liquid flow, and only release when they reached the liquid surface as seen by the red bubbles distribution in Figure 11 and the numerical graph in Figure 12.

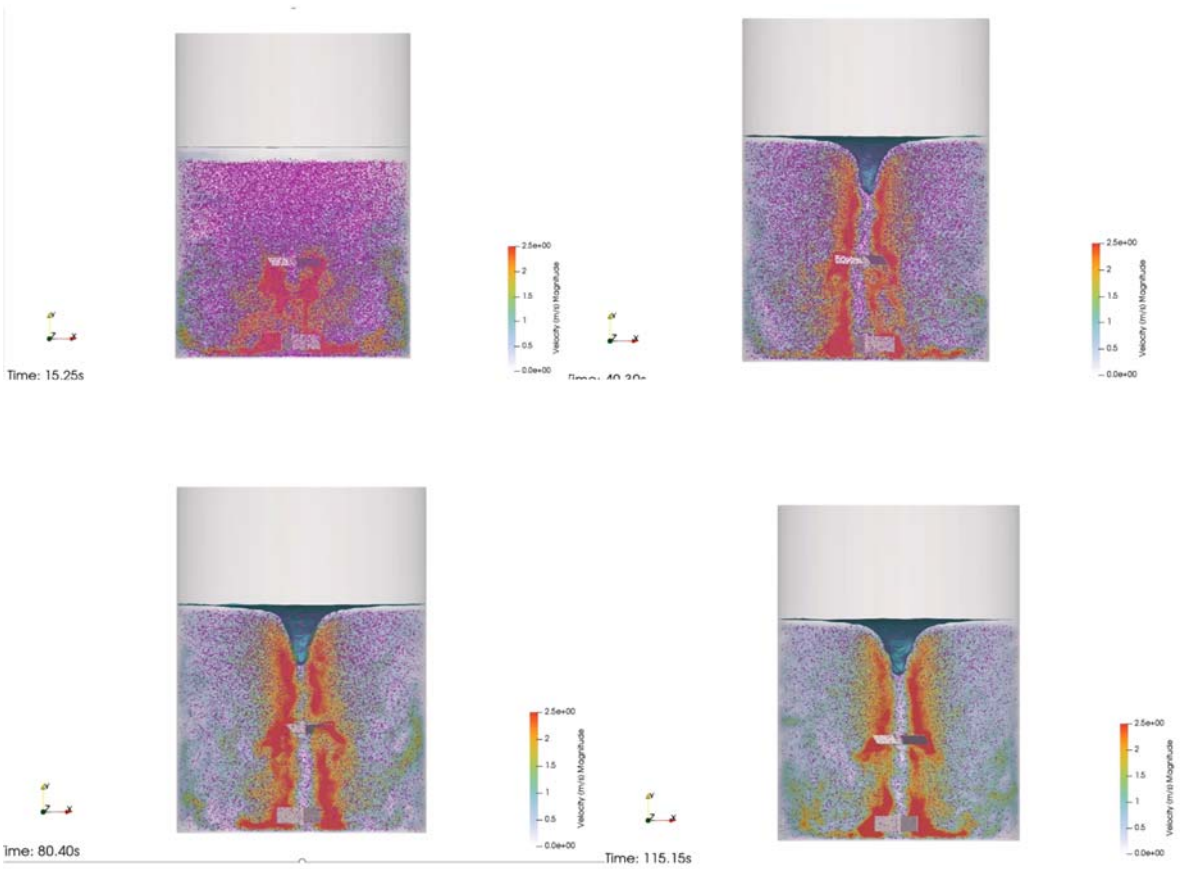

Figure 11. MSTAR CFD Simulation of Gas Bubble Release from SRAT Type Vessel

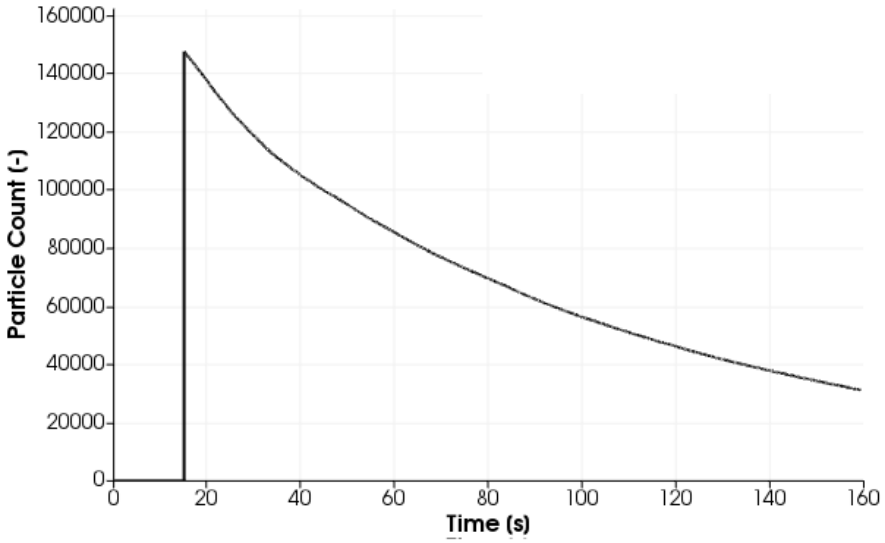

Figure 12. Bubble Count in SRAT Type Vessel

5.0 Conclusions

The conclusions from this study follow.

- The review of the technical literature describing the blending of Newtonian fluids and non-Newtonian fluids shows the mixing/blending to be a very fast process. In most instances the mixing time was less than 2 minutes. Investigating the mixing time in the SRAT and SME is unlikely to provide the data needed to relax the assumptions on instantaneous release of hydrogen upon the start of agitation, and the focus of the investigation is on hydrogen release rather than mixing time. Therefore, no further investigation of mixing/blending time is recommended.

- The literature on gas release from non-Newtonian fluids under quiescent conditions suggests a critical yield stress exists above which gas bubbles will not be released and below which gas bubbles will be released. The search also identified work in which hydrogen retention was a function of depth, but the work did not discuss the mechanism for the effect. Several investigators observed quiescent releases of gas bubbles. Included in the work observing quiescent release of hydrogen gas is data from the DWPF, SRNL data from DWPF sludge batch qualification, and the SRS Tank Farm. In assessing the quiescent release of gas from DWPF slurries, the slurry property of importance is the shear strength.

- Tank Farm data measuring the release of hydrogen during mixing with slurry pumps showed the hydrogen release to occur over several hours rather than instantaneously. Because of differences in agitation intensity, agitation method, vessel volume, headspace volume, purge rate, and power input, this data cannot be directly applied to the DWPF.

- SRNL sludge batch qualification testing showed retained hydrogen was released over several minutes rather than instantaneously upon startup of agitation. Because of differences in agitation intensity, vessel volume, headspace volume, purge rate, and power input, this data cannot be directly applied to the DWPF. Nevertheless, the data provides confidence that a release rate slower than instantaneous is valid for the SRAT and SME vessels.

- Previous work by SRNL and PNNL measured the rheology of Hanford sludge, and showed the rheology to increase as the sludge is allowed to settle. Changes in sludge rheology need considered when assessing changes to the DWPF retained hydrogen program.

- A comparison of buoyancy and inertial forces under SRAT operating conditions (1 – 10 Pa yield stress, 1.38 g/mL density, 65 or 130 rpm, 9,000 gallons of feed) on the bubbles (approximated as 300 microns diameter) found the inertial forces to be more than 350,000 times larger than the buoyancy forces. With this ratio of forces, the gas bubbles generated will follow the fluid motion in the SRAT, and only release when they reach the slurry-vapor interface.

- An informal Lattice Boltzmann Computation Fluid Dynamics calculation was performed on a SRAT type vessel. The liquid had a density of 1 g/mL and a viscosity of 20 cP. In the simulation, approximately 50% of the bubbles were released to the vapor space over ~80 seconds. The simulation showed the bubbles to follow the liquid flow, and only release when they reached the liquid surface.

6.0 Future Work

The authors recommend the following work be performed to assess the conservatism in the retained hydrogen program.

- Measuring quiescent hydrogen release from actual SRS waste.
- Measuring agitated hydrogen release from actual SRS waste.
- Modeling gas bubble release from SRS waste using Lattice-Boltzmann CFD software.
- Analyzing DWPF process data to better understand release rates at the DWPF.
- Conducting gas release tests with simulant to assist in the design of actual waste tests and the validation of the Lattice-Boltzmann CFD model.
- Performing rheology measurements to understand the impact of settling time on slurry rheology.
- Testing performed should include feeds representative of the DWPF contents with the glycolic acid flowsheet.

The quiescent release testing will use existing sludge samples at SRNL allowed to sit unagitated and measure the release of hydrogen that is generated by radiolysis. The rheology (i.e., shear strength) of the sludge will be measured prior to testing and varied during testing to understand its impact on hydrogen retention and release. Vessel height and diameter will be varied to understand their influence on hydrogen retention and release.

The agitated release tests will resemble the batch qualification tests performed previously but will focus on hydrogen release following restart of agitation after a process stoppage.

Personnel will use the Lattice Boltzmann CFD software to model previous SRNL data and DWPF data. The effort will fit the data by varying operating parameters such as bubble size, bubble concentration, rheology, and agitation to understand how these parameters affect the gas retention and release. In addition, the modeling can be used to help define parameters for the testing to be performed.

DWPF has measured hydrogen concentrations in the purge gas, and this information has been reported in summary form. An effort should be started to examine the raw data to determine if it can provide quantifiable information on the hydrogen release rate as a function of operating parameters. This effort should include collecting additional data moving forward.

Agitated release tests with simulant should be considered to aid in the design of actual waste tests in the SRNL Shielded Cells and the validation of the Lattice-Boltzmann CFD model.

Rheology measurements should be performed with actual waste to understand how properties such as yield stress and shear strength increase with settling time and how quickly the yield stress and shear strength recover following the loss of agitation.

More details on the testing and modeling will be included in the Task Technical and Quality Assurance Plan.

7.0 References

[1] "Defense Waste Processing Facility: System Design Description Sludge Feed Preparation System, CH-01", G-SYD-S-00054, Rev 11, May 2009.
[2] R. R. Hemrajani and G. B. Tatterson, "Mechanically Stirred Vessels", in E. L. Paul, V. A. Atiemo-Obeng, and S. M. Kresta, Eds., Handbook of Industrial Mixing: Science and Practice, Hoboken, Wiley, 2004.
[3] A. T. Clare, "Quiescent Time Evaluation Guidance Evaluation for DWPF Vessels", X-ESR-S-00282, July 26, 2016.
[4] M. C. Clark, "Retained Hydrogen Literature Study for Defense Waste Processing Facility (DWPF)", X-TAR-S-00009, October 2, 2018.
[5] SRNL-STI-2013-00299, Rev. 0, "Rheology and TiC/TOC Results of ORNL Tank Samples", Pareizs, J.M. and Hansen, E.K., April 2013
[6] SRNL-STI-2012-00519, Rev. 0, "2012 SRNL-EM Vane Rheology Results", Hansen, E.K., Marzolf, A.D., and Hera, K.R., August 2012
[7] T. P. Elson, D. J. Cheesman, and A. W. Nienow, "X-Ray Studies of Cavern Sizes and Mixing Performance with Fluids Possessing a Yield Stress", Chem. Eng. Sci., vol. 41, no. 10, pp. 2555-2562, 1986.
[8] T. P. Elson, "The Growth of Caverns Formed Around Rotating Impellers During the Mixing of a Yield Stress Fluid", Chem. Eng. Comm., vol. 96, pp. 303-319, 1990.
[9] A. W. Etchells, W. N. Ford, and D. G. R. Short, "Mixing of Bingham Plastics on an Industrial Scale", Fluid Mixing III: The Institution of Chemical Engineers Symposium Series No. 108, pp. 271-285, 1987.
[10] J. J. Derksen, "Blending of Miscible Liquids with Different Density Starting from Stratefied State", Competers and Fluids, vol 50, 2011, pp. 35-45.
[11] P. R. Gogate and A. B. Pandit, "Mixing miscible Liquids with Density Differences: Effect of Volume and Density of the Tracer Fluid", Can J Chem Eng, vol 77, 1999, pp. 988-996.
[12] G. R. Kasat and A. B. Pandit, "Mixing Time Studies in Multiple Impeller Agitated Tanks", Can J Chem Eng, vol 82, 2004, pp. 892-904.
[13] I. Houcine, E. Plasari, and R. David, "Effects of the Stirred Tank's Design on Power Consumption and Mixing Time in Liquid Phase", Chem Eng Technol, vol 23, 2000, pp. 605-613.
[14] R. K. Grenville and J. N. Tilton, "Jet Mixing in Tall Tanks: Comparison of Methods for Predicting Blending", Chem Eng Res Des, vol 89, 2011, pp. 2501-2506.
[15] R. K. Grenville and J. N. Tilton, "A New Theory Improves the Correlation of Blend Time Data from Turbulent Jet Mixed Vessels", Trans IChemE, Vol 74, Part A, 1996, pp. 390-396.
[16] R. K. Grenville and A. W. Nienow, "Blending of Miscible Liquids", in E. L. Paul, V. A. Atiemo-Obeng, and S. M. Kresta, eds., Handbook of Industrial Mixing: Science and Practice, Hoboken: Wiley, 2004.
[17] R. Grenville, "Blending of Viscous Newtonian and Pseudoplastic Fluids", PhD Thesis, Cranfield Institute of Technology, 1992.
[18] I. Ihejirika, "Mixing Time in Yield Stress Fluids", Thesis, Ryerson University, 2007.

[19] S. G. Farah Abadi, "The Role of Rheology in the Flow and Mixing of Complex Fluids", Thesis, University of Birmingham, 2016.
[20] L. Pakzad, F. Ein-Mozaffan, and P. Chan, "Measuring Mixing Time in the Agitation of Non-Newtonian Fluids through Electrical Resistance Tomography", Chem Eng Tech, vol 31, No. 12, 2008, pp. 1838-1845.
[21] L. Pakzad, F. Ein-Mozaffan, and P. Chan, "Using Electrical Resistance Tomography and Computational Fluid Dynamics Modeling to Study the Formation of Cavern in the Mixing of Pseudoplastic Fluids Possessing Yield Stress", Chem Eng Sci, vol 63, 2008, pp. 2508-2522.
[22] R. Grenville, "Blending of Viscous Newtonian and Pseudoplastic Fluids", PhD Thesis, Cranfield Institute of Technology, 1992.
[23] G. Montante, M. Mostek, M. Jahoda, and F. Magelli, "CFD Simulations and Experimental Validation of Homogenisation Curves using Mixing Time in Stirred Newtonian and Pseudoplastic Liquids", Chem Eng Sci, vol 60, 2005, pp. 2427-2437.
[24] W. Adams and M. Barigou, "CFD Analysis of Caverns and Pseudocaverns Developed During Mixing of Non-Newtonian Fluids", Chem Eng Res Des, vol 85, 2007, pp. 598-604.
[25] N. Nimalkar, A. K. Gupta, and R. P. Chhabra, "Natural Convection from a Heated Sphere in Bingham Plastic Fluids", I and EC Research, vol 53, 2014, pp. 17818-17832
[26] D. Sikorski, H. Tabuteau, and J. R. de Bruyn, "Motion and Shape of Bubbles Rising through a Yield Stress Fluid", J non-Newtonian Fluid Mech, vol. 159, 2009, pp. 10-16
[27] J. Tsamopoulos, Y. Dimakopoulos, N. Chatzidal, G. Karapetsas, and M. Pavlidis, "Steady Bubble Rise and Deformation in Newtonian and Viscoplastic Fluids and Conditions for Bubble Entrapment", J Fluid Mech, vol 601, 2008, pp. 123-164.
[28] Y. Dimakopoulos, M. Pavlidis, and J. Tsamopoulos, "Steady Bubble Rise in Herschel-Bulkley Fluids and Comparison of Predictions via the Augmented Lagrangian Method with those via the Papanastasiou Model", J non-Newtonian Fluid Mech, vol 200, 2013, pp. 34-51.
[29] N. Dubash and I. A. Frigaard, "Propagation and Stopping of Air Bubbles in Carbopol Solutions", J non-Newtonian Fluid Mech,, vol 142, 2007, pp. 123-134.
[30] A. E. Papathanassiu, H. Abramowitz, N. Mecholsky, R. Cecil, and I. L. Pegg, "Gas Retention and Release Studies for DWPF Phase II", VSL-17R3850-1.
[31] X. Frank, N. Dietrich, J. Wu, R. Barraud, and H. Z. Li, "Bubble Nucleation and Growth in Fluids", Chem Eng Sci, vol 62, 2007, 7090-7097.
[32] A. T. Clare, "Safety Analysis Input: Hydrogen Retention Fraction", DWPF-I-RG-0001.
[33] L. A. Ledbetter, "Hydrogen Retention Rates in Slurried Sludge", WSRC-TR-2004-00077, Rev 0.
[34] M. J. Ades, "Hydrogen Retention Rates in Slurried Sludge", WSRC-TR-2004-00077, Rev 2.
[35] J. M. Pareizs, N. E. Bibler, and T. L. Fellinger, "Radiolytic Hydrogen Generation and Retention in Tank 40 (Sludge Batch 3) Sludge", WSRC-TR-2005-00555.
[36] A. T. Clare, "Safety Analysis Input: Bubble Gas Volume Percent in DWPF Sludge", DWPF-I-RG-0002.
[37] D. J. Sherwood and A. E. Saez, "The Start of Ebullition in Quiescent, Yield-Stress Fluids", Nuc Eng Des, vol. 270, 2014, pp. 101-108.
[38] A. E. Papathanassiu, H. Abramowitz, N. Mecholsky, R. Cecil, and I. L. Pegg, "Gas Retention and Release Studies for DWPF Phase II", VSL-17R3850-1.
[39] T. van Kessel and W. G. M. van Kesteren, "Gas Production and Transport in Artificial Sludge Depots", Waste Management, vol 22, 2002, pp. 19-28.
[40] M. Johnson, M. Fairweather, D. Harbottle, T. N. Hunter, J. Peakall, and S. Biggs, "Yield Stress Dependency on the Evolution of Bubble Populations Generated in Consolidated Soft Sediments", AIChE J vol 63, No. 9, 2017, pp. 3728-3742.
[41] J. R. Hester, "Hydrogen Release during Tank 40H and 8F Slurry Runs", WSRC-TR-2000-00366.
[42] J. R. Hester, "Hydrogen Accumulation and Release Behavior of Tank 40H Sludge Slurry", WSRC-TR-2003-00292.

[43] P. P. Schonewill et al., "Evaluation of Gas Retention in Waste Simulants: Tall Column Experiments", PNNL-23340.
[44] P. A. Gauglitz et al., "Strong-Sludge Gas Retention and Release Mechanisms in Clay Simulants", PNNL-21167.
[45] I. Bodey, "On the Evaluation of the Retention and Release of Catalytically Generated Hydrogen Gas in Slurries Associate with the Defense Waste Processing Facility", X-ESR-S-00265, Rev 0, September 15, 2015.
[46] J. M. Pareizs, B. R. Pickenheim, C. J. Bannochie, A. L. Billings, N. E. Bibler, and D. R. Click, "Sludge Washing and Demonstration of the DWPF Flowsheet in the SRNL Shielded Cells for Sludge Batch 6 Qualification", SRNL-STI-2010-00353.
[47] J. M. Pareizs, A. L. Billings, and D. R. Click, "Sludge Washing and Demonstration of the DWPFFlowsheet in the SRNL Shielded Cells for Sludge Batch 7a Qualification", SRNL-STI-2011-00226.
[48] J. M. Pareizs, A. L. Billings, S. H. Reboul, D. P. Lambert, and D. R. Click, "Sludge Batch 7b Qualification Activities with SRS Tank Farm Sludge", SRNL-STI-2011-00548.
[49] J. M. Pareizs, C. J. Bannochie, D. R. Click, D. P. Lambert, M. E. Stone, B. R. Pickenheim, A. L. Billings, and N. E. Bibler, "Sludge Washing and Demonstration of the DWPF Flowsheet in the SRNL Shielded Cells for Sludge Batch 5 Qualification", SRNS-STI-2008-00111, November 2008.
[50] J. M. Pareizs and C. L. Crawford, "Sludge Washing and Demonstration of the DWPF Flowsheet in the SRNL Shielded Cells for Sludge Batch 8 Qualification", SRNL-STI-2011-00116, April 2013.
[51] J. M. Pareizs, C. J. Bannochie, D. R. Click, D. P. Lambert, M. E. Stone, B. R. Pickenheim, A. L. Billings, and N. E. Bibler, "Sludge Washing and Demonstration of the DWPF Flowsheet in the SRNL Shielded Cells for Sludge Batch 5 Qualification", SRNS-STI-2008-00111, November 2008.
[52] M. C. Clark, "Retained Hydrogen Literature Study for Defense Waste Processing Facility (DWPF)", X-TAR-S-00009, October 2, 2018.
[53] G. S. Kinsley, "Properly Purge Inert Storage Vessels", Chem Eng Prog, Feb 2001, pp. 57-61.
[54] M. S. Hay and E. D. Lee, "Hydrogen Evolution and Sludge Suspension During the Preparation of the First Batch of Sludge at the Savannah River Site", WSRC-MS-94-0541, Waste Management '95 Meeting, Tucson, AZ, February 26 – March 2, 1995.
[55] Kalaichelvi, P, Swarnalatha, Y., and Raja, T., "Mixing Time Estimation and Analysis in a Jet Mixer", ARPN Journal of Engineering and Applied Sciences, Vol. 2, No. 5, October 2007.
[56] M. R. Poirier, "Mixing in Closure Business Unit Applications", WSRC-TR-2004-00153, March 30, 2004.
[57] R. A. Leishear, M. R. Poirier, and M. D. Fowley, "Blending Study for SRR Salt Disposition Integration: Tank 50H Scale Modeling and Computer Modeling for Blending Pump Design, Phase 2", SRNL-STI-2011-00151, May 2011.
[58] R. Patel, G. Tachiev, N. Yadaz, A. Awwad, D. McDaniel, and D. Roelant, "Gas Retaining and Release Experiments with Low Yield Stress Fluids", Paper 11289, Waste Management 2011, Phoenix, AZ.
[59] Rassat, S.D., Caley, S.M., Bredt, P.R., Gauglitz, P.A., Rinehart, D. E., and Forbes, S.V., "Mechanisms of Gas Retention and Release: Experimental Results for Hanford Single-Shell Waste Tanks 241-A-101, 241-S-106, and 241-U-103", PNNL-11981, September 1998.
[60] Liddell, P.V. and Boger, D. V., "Yield stress measurements with the vane", Journal of non-Newtonian Fluid Mechanics', Vol. 63, pp. 235-261, 1996.
[61] Nguyen, Q.D., Akroyd, T., De Kee, D. C., and Zhu, L., "Yield stress measurements in suspensions: an inter-laboratory study", Korea-Australis Rheology Journal, Vol. 18, pp. 15-24, 2006.
[62] Hansen, E. and Crawford, C., "Hanford HLW AY106/C106 Pretreated Sludge Physical and Chemical Properties Prior to Melter Feed Processing", WSRC-TR-2004-00394, Rev. 1, 2006.
[63] Pareizs, J.M. and Hansen, E. K., "Rheology and TIC/TOC Results of ORNL Tank Samples", SRNL-STI-2013-00299, 2013.
[64] Poloski, A.P., Bredt, P.R., Chenault, J.W., and Swobada, R.G., "Rheological and Physical Properties of AZ-101 HLW Pretreated Sludge and Melter Feed", WTP-RPT-096, 2003.

[65] Tingey, J., Gao, J., Delegard, C., Bagaasen, L., and Wells, B, "Physical Property and Rheological Testing of Actual Transuranic Waste from Hanford Single-Shell Tanks", PNNL-14365, 2003.
[66] V. Machon, A. W. Pacek, A. W. Nienow, "Bubble Sizes in Electrolyte and Alcohol Solutions in a Turbulent Stirred Vessel", Trans IChemE, vol. 75, Part A, 1997, pp. 339-348.
[67] J. Eshraghi, E. Kosari, P. Hadikhani, A. Amini, M. Ashjaee, "Numerical Study of Surface Tension Effects on Bubble Detachment in a Submerged Needle", WIT Transactions on Engineering Sciences, vol 89, 2015, pp. 77-86.
[68] E. W. Washburn, Ed., International Critical Tables of Numerical Data, Physics, Chemistry and Technology, New York: McGraw-Hill, 1929.

Distribution:

timothy.brown@srnl.doe.gov
alex.cozzi@srnl.doe.gov
david.crowley@srnl.doe.gov
c.diprete@srnl.doe.gov
a.fellinger@srnl.doe.gov
samuel.fink@srnl.doe.gov
nancy.halverson@srnl.doe.gov
erich.hansen@srnl.doe.gov
connie.herman@srnl.doe.gov
Joseph.Manna@srnl.doe.gov
john.mayer@srnl.doe.gov
daniel.mccabe@srnl.doe.gov
Gregg.Morgan@srnl.doe.gov
frank.pennebaker@srnl.doe.gov
Amy.Ramsey@srnl.doe.gov
William.Ramsey@SRNL.DOE.gov
michael.stone@srnl.doe.gov
Boyd.Wiedenman@srnl.doe.gov
bill.wilmarth@srnl.doe.gov
Records Administration (EDWS)

jeffrey.crenshaw@srs.gov
james.folk@srs.gov
roberto.gonzalez@srs.gov
tony.polk@srs.gov
patricia.suggs@srs.gov
Michael Poirier
Mark Duignan

Kevin.Brotherton@srs.gov
Richard.Edwards@srs.gov
terri.fellinger@srs.gov
eric.freed@srs.gov
jeffrey.gillam@srs.gov
barbara.hamm@srs.gov
bill.holtzscheiter@srs.gov
john.iaukea@srs.gov
Vijay.Jain@srs.gov
chris.martino@srnl.doe.gov
jeff.ray@srs.gov
paul.ryan@srs.gov
Azadeh.Samadi-Dezfouli@srs.gov
hasmukh.shah@srs.gov
aaron.staub@srs.gov
thomas.colleran@srs.gov
Spencer.Isom@srs.gov
MARIA.RIOS-ARMSTRONG@SRS.GOV
Mason.Clark@srs.gov
Jeremiah.Ledbetter@srs.gov
Grace.Chen@srs.gov
Jocelin.stevens@srs.gov